NOAA Technical Report NESS 85

Transmittances for the TIROS Operational Vertical Sounder

Washington, D.C.
September 1981

U.S. DEPARTMENT OF COMMERCE
National Oceanic and Atmospheric Administration
National Earth Satellite Service

NOAA TECH REPORTS

National Earth Satellite Service Series

The National Earth Satellite Service (NESS) is responsible for the establishment and operation of the environmental satellite systems of NOAA.

Publication of a report in NOAA Technical Report NESS series will not preclude later publication in an expanded or modified form in scientific journals. NESS series of NOAA Technical Reports is a continuation of, and retains the consecutive numbering sequence of, the former series, ESSA Technical Report National Environmental Satellite Center (NESC), and of the earlier series, Weather Bureau Meteorological Satellite Laboratory (MSL) Report. Reports 1 through 39 are listed in publication NESC 56 of this series.

Reports in the series are available from the National Technical Information Service (NTIS), U.S. Department of Commerce, Sills Bldg., 5285 Port Royal Road, Springfield, VA 22161, in paper copy or microfiche form. Order by accession number, when given, in parentheses. Beginning with 64, printed copies of the reports, if available, can be ordered through the Superintendent of Documents, U.S. Government Printing Office, Washington, DC 20402. Prices given on request from the Superintendent of Documents or NTIS.

ESSA Technical Reports

NESC 46 Monthly and Seasonal Mean Global Charts of Brightness From ESSA 3 and ESSA 5 Digitized Pictures, February 1967–February 1968. V. Ray Taylor and Jay S. Winston, November 1968, 9 pp. plus 17 charts. (PB-180-717)

NESC 47 A Polynomial Representation of Carbon Dioxide and Water Vapor Transmission. William L. Smith, February 1969 (reprinted April 1971), 20 pp. (PB-183-296)

NESC 48 Statistical Estimation of the Atmosphere's Geopotential Height Distribution From Satellite Radiation Measurements. William L. Smith, February 1969, 29 pp. (PB-183-297)

NESC 49 Synoptic/Dynamic Diagnosis of a Developing Low-Level Cyclone and Its Satellite-Viewed Cloud Patterns. Harold J. Brodrick and E. Paul McClain, May 1969, 26 pp. (PB-184-612)

NESC 50 Estimating Maximum Wind Speed of Tropical Storms From High Resolution Infrared Data. L. F. Hubert, A. Timchalk, and S. Fritz, May 1969, 33 pp. (PB-184-611)

NESC 51 Application of Meteorological Satellite Data in Analysis and Forecasting. Ralph K. Anderson, Jerome P. Ashman, Fred Bittner, Golden R. Farr, Edward W. Ferguson, Vincent J. Oliver, Arthur H. Smith, James F. W. Purdom, and Rance W. Skidmore, March 1974 (reprint and revision of NESC 51, September 1969, and inclusion of Supplement, November 1971, and Supplement 2, March 1973), pp. 1--6C-18 plus references.

NESC 52 Data Reduction Processes for Spinning Flat-Plate Satellite-Borne Radiometers. Torrence H. MacDonald, July 1970, 37 pp. (COM-71-00132)

NESC 53 Archiving and Climatological Applications of Meteorological Satellite Data. John A. Leese, Arthur L. Booth, and Frederick A. Godshall, July 1970, pp. 1-1--5-8 plus references and appendixes A through D. (COM-71-00076)

NESC 54 Estimating Cloud Amount and Height From Satellite Infrared Radiation Data. P. Krishna Rao, July 1970, 11 pp. (PB-194-685)

NESC 56 Time-Longitude Sections of Tropical Cloudiness (December 1966-November 1967). J. M. Wallace, July 1970, 37 pp. (COM-71-00131)

NOAA Technical Reports

NESS 55 The Use of Satellite-Observed Cloud Patterns in Northern Hemisphere 500-mb Numerical Analysis. Roland E. Nagle and Christopher M. Hayden, April 1971, 25 pp. plus appendixes A, B, and C. (COM-73-50262)

NESS 57 Table of Scattering Function of Infrared Radiation for Water Clouds. Giichi Yamamoto, Masayuki Tanaka, and Shoji Asano, April 1971, 8 pp. plus tables. (COM-71-50312)

NESS 58 The Airborne ITPR Brassboard Experiment. W. L. Smith, D. T. Hilleary, E. C. Baldwin, W. Jacob, H. Jacobowitz, G. Nelson, S. Soules, and D. Q. Wark, March 1972, 74 pp. (COM-72-10557)

NESS 59 Temperature Sounding From Satellites. S. Fritz, D. Q. Wark, H. E. Fleming, W. L. Smith, H. Jacobowitz, D. T. Hilleary, and J. C. Alishouse, July 1972, 49 pp. (COM-72-50963)

NESS 60 Satellite Measurements of Aerosol Backscattered Radiation From the Nimbus F Earth Radiation Budget Experiment. H. Jacobowitz, W. L. Smith, and A. J. Drummond, August 1972, 9 pp. (COM-72-51031)

(Continued on inside back cover)

NOAA Technical Report NESS 85

Transmittances for the TIROS Operational Vertical Sounder

M.P. Weinreb, H.E. Fleming,
L.M. McMillin, and A.C. Neuendorffer

Washington, D.C.
September 1981

U.S. DEPARTMENT OF COMMERCE
Malcolm Baldrige, Secretary

National Oceanic and Atmospheric Administration
John V. Byrne, Administrator

National Earth Satellite Service
David S. Johnson, Assistant Administrator for Satellites

National Oceanic and Atmospheric Administration
TIROS Satellites and Satellite Meteorology

CONTENTS

TABLES

FIGURES

Transmittances for the TIROS Operational Vertical Sounder

M.P. Weinreb, H.E. Fleming, L.M. McMillin, and A.C. Neuendorffer

Office of Research
National Earth Satellite Service/NOAA
Washington, D.C. 20233

ABSTRACT. We describe how atmospheric transmittances are calculated for temperature soundings with the TIROS Operational Vertical Sounder (TOVS). The role of transmittances in both integrating and solving the radiative transfer equation is discussed. Our transmittance calculations satisfy the dual requirements of operational data processing: accuracy and efficiency. Transmittances are generated for vertical and slant paths. They represent convolutions with the spectral response functions of the infrared and the microwave channels of the TOVS. For spectral lines of the uniformly-mixed gases and of water vapor, efficient approximations are used in lieu of "exact", but time-consuming line-by-line calculations. The water-vapor continua and molecular nitrogen's 4.3-μm band are integrated directly through the atmosphere. A simple interpolation scheme suffices for the weak absorption by ozone. Absorption by oxygen and water vapor in the 55-GHz region is approximated. We conclude by presenting graphs of calculated profiles of transmittances vs altitude.

1. INTRODUCTION

This report documents how atmospheric transmittances are calculated in the processing system for the TIROS Operational Vertical Sounder (TOVS) at the National Earth Satellite Service (NESS). The TOVS (Schwalb 1978, Smith et al. 1979) comprises three radiometers operating in the infrared and microwave portions of the spectrum and is dedicated to measuring remotely vertical profiles of atmospheric temperature and humidity. Currently, these profiles are retrieved from the measured radiances with statistical regression techniques (Smith and Woolf 1976), which do not use transmittances. However, transmittances are used off line[1] to generate dependent samples of data for the statistical algorithms that "correct" radiances for

[1]The term "off line" refers to computer programs that are run infrequently, e.g., before launch of each TOVS, or at most once every two weeks. They are not part of the processing system that provides retrievals orbit by orbit in near real time. Off-line programs develop coefficients to be used in the orbit-by-orbit (or "on-line") processing, and they may consume more computer time than is available during on-line processing.

variation with viewing angle and remove the effects of water vapor in window channels. In the future, the role of the transmittances may be expanded with the introduction of the "minimum-information" method of retrieval (Fleming and Smith 1972) into the operational system. This method solves the radiative transfer equation and requires transmittances to be computed on line. Transmittances also find application in the processing of TOVS data received at direct read-out stations and other installations outside of NESS. Therefore, while this report is motivated simply by the need to document the transmittance calculations in use at NESS, one of its uses may be to assist scientists at other locations in setting up their own processing systems.

Transmittances are calculated at NESS for 21 of the 22 infrared channels and for all four microwave channels of the TOVS. In each channel we calculate a profile of transmittances, i.e., values of transmittance at 40 atmospheric pressure levels, which correspond to 40 altitudes. The transmittances are specific to the TOVS channels, because they are convolutions of atmospheric transmittances with the spectral response functions (transmission vs frequency or wavenumber) that define each channel. The spectral widths (full widths at half-maximum) of these functions vary from channel to channel, with values ranging from about 3 cm^{-1} to 100 cm^{-1} in the infrared channels. The widths are 220 GHz in all the microwave channels (Schwalb 1978).

Transmittances are computed for the TOVS by a complex, multi-algorithm procedure. Atmospheric transmittances are assumed to be the product of transmittances of each absorbing constituent. For each constituent, transmittances are associated with either spectral lines (e.g. carbon dioxide) or broad spectral features (e.g. molecular nitrogen), or, the case of water vapor, with both. For spectral lines, we have developed simple but highly accurate parameterizations to substitute for the cumbersome, brute-force, but "exact" procedure of computing transmittances line by line and convolving them with spectral response functions. (Although other simple models are available, e.g. LOWTRAN (Kneizys et al. 1980), we did not use them because they are neither specific to the various filter profiles of TOVS nor accurate enough for our application.) Our parameterizations allow the on-line calculations to consume as little time as possible. Meanwhile, the line-by-line calculations and convolutions, which are still required for producing coefficients for the parameterizations, are relegated to off-line status.

Although some of the algorithms in this report have already been published elsewhere, we describe them here for completeness. Such material is presented only in outline, and for details the reader is referred to the original manuscripts. On the other hand, material not documented elsewhere is described fully here. For these reasons the reader will note that the depth of the explanation varies from one section to another in this report.

This report does not list the coefficients used in any of the algorithms. Most of the algorithms require only a few coefficients, but one (see section 3.2.1) requires 320 per channel and is applied in 19 channels, making 6080 coefficients in all. Furthermore, each TOVS instrument has its own complete set of coefficients, so that, for example, we use one set of coefficients for the TOVS on TIROS-N and another set for TOVS on NOAA-6. Obviously, a full tabulation of these coefficients would be too much for this report. Instead, we have put all the coefficients on a magnetic tape, copies of which are available from the Satellite Data Services Division, Environmental Data and Information Service, National Oceanic and Atmospheric Administration, World Weather Building, Washington, D.C. 20233. This tape also contains the on-line FORTRAN source code that implements the algorithms described in this report. With this tape a user has all he needs to compute transmittances for TOVS by the techniques used at NESS.

2. BACKGROUND

2.1 The TIROS Operational Vertical Sounder

Atmospheric soundings are extracted from measurements made by the three instruments that comprise the TIROS Operational Vertical Sounder (TOVS). These instruments are the High Resolution Infrared Radiation Sounder (HIRS), the Microwave Sounding Unit (MSU), and the Stratospheric Sounding Unit (SSU). They are described by Schwalb (1978). The primary instrument is the HIRS. It is a filter radiometer, having seven channels in the 15 μm region and five channels in the 4.3-μm region. These are used in inferring atmospheric temperatures. It also has three "window" channels that sense in spectral intervals where the atmosphere is nearly transparent, three channels near 7 μm for measuring atmospheric water vapor, one channel at 9.7 μm for measuring ozone, and one channel at .69 μm in the visible spectrum for measuring the earth's albedo. Table 1 summarizes the characteristics of these channels. The last column in table 1 refers to the pressure at the approximate middle of the atmospheric layer that contributes the radiation in each channel.

The HIRS measures radiation welling up from the earth's atmosphere as it scans across the satellite's track, defining 56 fields of view per scan. At the outermost fields of view, the satellite's local zenith angle is just under 60°.

Table 1.--Characteristics of HIRS sounding channels

HIRS channel number	Central wavenumber (cm^{-1})	Central wavelength (μm)	Half-power bandwidth (cm^{-1})	Level of peak energy contribution
1	668	15.00	3	30 mb
2	679	14.70	10	60 mb
3	691	14.50	12	100 mb
4	704	14.20	16	400 mb
5	716	14.00	16	600 mb
6	732	13.70	16	800 mb
7	748	13.40	16	900 mb
8	898	11.10	35	Surface
9	1028	9.70	25	25 mb
10	1217	8.30	60	900 mb
11	1364	7.30	40	700 mb
12	1484	6.70	80	500 mb
13	2190	4.57	23	1000 mb
14	2213	4.52	23	950 mb
15	2240	4.46	23	700 mb
16	2276	4.40	23	400 mb
17	2361	4.24	23	5 mb
18	2513	4.00	35	Surface
19	2671	3.70	100	Surface
20	14367	0.70	900	Cloud

A problem with temperature sounding in the infrared is that the measured radiances are corrupted if clouds are present. To help overcome this, the HIRS is supplemented by the MSU, which has one window channel and three channels in the oxygen band near 60 GHz. Although MSU measurements are attenuated in areas of heavy precipitation, they are unaffected by most clouds. In partly cloudy areas the MSU data are used to alleviate the effects of clouds in the HIRS measurements, while in the overcast areas they provide the only information about the atmosphere below the clouds. Table 2 summarizes the spectral characteristics of the MSU. The MSU's field of view is much larger than the HIRS's, and it has only eleven fields of view in a cross-track scan. An area covered by an array of 56 (cross track) x 40 (along the track) HIRS measurements is also covered by an 11 x 10 array of MSU measurements.

Table 2.--Characteristics of MSU sounding channels

MSU	Frequency (GHz)	Half-power bandwidth (MHz)	Level of peak energy contribution
1	50.31	220	Surface
2	53.73	220	700 mb
3	54.96	220	300 mb
4	57.95	220	90 mb

For measurements in the upper atmosphere, the HIRS is supplemented by the SSU, which consists of three Pressure Modulated Radiometers (PMR's) (Miller et al. 1980). The PMR's isolate radiation originating near the centers of carbon dioxide lines by viewing the atmosphere through cells of carbon dioxide whose internal pressures are modulated with oscillating pistons. Filters in the optical path confine the radiation to an approximately 60-cm^{-1}-wide interval in the 15-μm band of carbon dioxide. The altitude regimes to be sensed are selected by the choices of the path length and mean pressure of gas in each cell. The spectral characteristics of the SSU appear in table 3. This instrument has a larger field of view than even the MSU. However, it does not scan to the extremes of the HIRS scan. The 8 x 8 array of SSU measurements covers only a 42 x 40 array of HIRS measurements.

Table 3.--Characteristics of SSU sounding channels

SSU	Central wavenumber (cm^{-1})	Central wavelength (μm)	Half-power bandwidth* (cm^{-1})	Cell pressure (mb)	Level of peak energy contribution
1	665	15	60	100	15.0 mb
2	665	15	60	35	4.0 mb
3	665	15	60	10	1.5 mb

*Bandwidth of filters alone. Pressure modulation further restricts effective bandwidth.

2.2 Transmittances in the Kernel of the Radiative Transfer Equation

This section illustrates how transmittances are involved in the problem of retrieving atmospheric temperature profiles from measurements of radiances. In the process, it shows how the transmittances must be averaged over the spectral response functions of radiometers.

2.2.1 Infrared Region

The theoretical basis for the retrieval of vertical profiles of temperature and humidity from infrared radiances measured by the TOVS is the integral form of the radiative transfer equation. As applied to a plane-parallel atmosphere in local thermodynamic equilibrium with no scattering, it is given by

$$I(\nu,\theta) = B(\nu, T_s)\ \tau(\nu,\theta, x_s) + \int_0^{x_s} B(\nu,T(x))\ \left(-\frac{d\tau(\nu,\theta, x)}{dx}\right) dx, \qquad (1)$$

where $I(\nu,\theta)$ is the monochromatic radiance welling up from the atmosphere at wavenumber ν and zenith angle θ, $B(\nu,T(x))$ is the Planck function at ν and temperature T, with the independent variable x a monotonically increasing function of pressure, and $\tau(\nu,\theta,x)$ is the fractional transmittance from the level x to the effective top of the atmosphere. The subscript "s" refers to the surface. Equation (1) shows that the radiance $I(\nu,\theta)$ has two components: (1) the contribution from the surface, determined by the first term on the right-hand side, which is known as the "boundary term," and (2) the contribution of the atmosphere, determined by the integral on the right-hand side.

As written, eq. (1) applies only to monochromatic radiation. However, measurements can only be made over finite spectral intervals. Furthermore, a satellite radiometer responds to radiation in a nonuniform way as a function of wavenumber. The instrument spectral response function (or spectral profile) may be denoted by $\phi(\nu)$. However, since the TOVS has 27 response functions, for the purpose of identification we also characterize each by an additional parameter, the wavenumber ν^* of the centroid of the response function. Hence, ϕ can be written as a function of the parameter ν^* as well as of the variable ν; that is, $\phi = \phi(\nu,\nu^*)$.

So that eq. (1) represents the outgoing radiance as viewed by a satellite, it must be: (1) multiplied by the response function ϕ; (2) normalized so that ϕ represents the weight in the weighted average; and (3) integrated over the interval of response ν_1 to ν_2. Thus, the measured radiance is given by

$$I(\nu^*,\theta) = \int_{\nu_1}^{\nu_2} \hat{\phi}(\nu,\nu^*)\ I(\nu,\theta)\ d\nu = \int_{\nu_1}^{\nu_2} \hat{\phi}(\nu,\nu^*)\ B\ (\nu, T_s)\ \tau(\nu,\theta,x_s)\ d\nu$$

$$+ \int_{\nu_1}^{\nu_2} \int_0^{x_s} \hat{\phi}(\nu,\nu^*)\ B(\nu, T(x))\ \left(-\frac{d\tau(\nu,\theta,x)}{dx}\right) dx\,d\nu, \qquad (2)$$

where $\hat{\phi}(\nu,\nu^*)$ is the normalized instrument response function given by

$$\hat{\phi}(\nu,\nu^*) = \phi(\nu,\nu^*)/\int_{\nu_1}^{\nu_2} \phi(\nu,\nu^*)\, d\nu.$$

When the second mean-value theorem for integrals is applied to eq. (2) and the order of integration is interchanged, one obtains the result,

$$\bar{I}(\nu^*,\theta) = B(\nu^*, T_s)\ \bar{\tau}(\nu^*,\theta, x_s) + \int_{o}^{x_s} B(\nu^*,T(x))\left(-\frac{d\bar{\tau}(\nu^*,\theta,x)}{dx}\right) dx, \quad (3)$$

where

$$\bar{\tau}(\nu^*,\theta, x) = \int_{\nu_1}^{\nu_2} \hat{\phi}(\nu,\nu^*)\ \tau(\nu,\theta, x)\, d\nu \quad (4)$$

and

$$\frac{d\bar{\tau}(\nu^*,\theta,\nu)}{dx} = \int_{\nu_1}^{\nu_2} \hat{\phi}(\nu,\nu^*)\ \frac{d\tau(\nu,\theta,x)}{dx}\, d\nu. \quad (5)$$

(Note that eq. (3) is only an approximation (but an accurate one) because $B(\nu^*,T)$ is not necessarily the mean value of B.) It is not convenient to compute the mean derivative of transmittance by eq. (5), but by Leibniz's rule it is also true that

$$\frac{d\bar{\tau}(\nu^*,\theta,\nu)}{dx} = \frac{d}{dx} \int_{\nu_1}^{\nu_2} \hat{\phi}(\nu,\nu^*)\ \ \tau(\nu,\theta,x)\, d\nu, \quad (6)$$

which by eq. (4) yields an efficient method for computing the derivative.

While eq. (3) is identical to eq. (1) in form, eq. (3) is for polychromatic radiation and involves the mean transmittance, defined and computed by eq. (4), and the mean derivative of transmittance, defined by eq. (5) and computed by eq. (6). In a typical temperature retrieval problem one solves eq. (3) for the temperature profile T as a function of pressure, based on knowledge of the measured radiance $\bar{I}(\nu^*,\theta)$ and the mean transmittance $\bar{\tau}(\nu^*,\theta,x)$. Thus, the atmospheric transmittance, which is of concern here, enters as an attenuating factor in the boundary term and as a weighting function in the integral term. It is the computation of equation (4) that represents the ultimate objective of this report.

When the Planck function is significantly non-linear across the spectral extent of the response function, as it is in the short-wavelength channels of the HIRS, eq. (3) may not be accurate with $\nu = \nu^*$, the centroid. Hence, an additional step, the defining of a profile of effective temperature $T_e(x)$ to replace the true temperature profile $T(x)$, is executed before eq. (3) is evaluated. This assumes that one can find an effective temperature profile such that eq. (3) is valid for $\nu = \nu^*$ when $T_e(x)$ replaces $T(x)$, and that T_e can be related to T and ν^*.

The introduction of the concept of an effective temperature in eq. (3) avoids the difficulties created by use of the mean-value theorem. In other words, from the theorem we know there exists a wavenumber $\hat{\nu}$ in the interval ν_1 to ν_2 such that eq. (3), together with eqs. (4) and (5), is valid whenever $\hat{\nu}$ replaces ν^*. But the value of $\hat{\nu}$ cannot be determined a priori. Furthermore, $\hat{\nu}$ depends on T, and since T depends on x, $\hat{\nu}$ varies with x. Thus, the strategy of using an effective temperature is to leave ν equated to the known centroid ν^* and instead to shift the burden of guaranteeing equality in eq. (3) to $T(x)$ by replacing it with $T_e(x)$.

The approach used to determine T_e from T and ν^* in the TOVS system, suggested by Smith and Abel (1974), is as follows. First, a set of 100 average blackbody radiances $\{\bar{I}_i(\nu^*)\}$ is calculated for a set of 100 temperatures $\{T_i\}$ from the integral

$$\bar{I}_i(\nu^*) = \int_{\nu_1}^{\nu_2} \hat{\phi}(\nu,\nu^*)\ B(\nu,T_i)\ d\nu. \tag{7}$$

Then the set of 100 effective temperatures $\{T_e(i)\}$ is determined from the blackbody temperatures of $\bar{I}_i(\nu^*)$, that is,

$$T_e(i) = B^{-1}\ [\nu^*,\ \bar{I}_i\ (\nu^*)], \tag{8}$$

where B^{-1} is the inverse Planck function with respect to temperature. Finally, a linear relationship of the form

$$T_i = a(\nu^*) + b(\nu^*)\ T_e(i) \tag{9}$$

is determined between the original and effective temperatures in which the coefficients are determined by ordinary least squares.

In the operational processing one integrates the radiative transfer equation by first computing $T_e(x)$ from $T(x)$ using the inverse of eq. (9) and then evaluating eq. (3) with $T(x)$ replaced by $T_e(x)$. Conversely, one solves the radiative transfer equation for $T_e(x)$ and then, as the final step in the retrieval process, converts to the true temperature profile $T(x)$ by eq. (9). (For a new approach that is more accurate than that of using effective temperatures, see Fleming (1981).)

2.2.2. Microwave Region

Recall that eq. (1), and hence eq. (3), is the form of the radiative transfer equation that is used in the infrared. Among other things, it assumes that the surface emissivity is unity. In the microwave region this assumption is not valid, and the radiative transfer equation must be modified accordingly. First, several minor changes are made. The variable ν now represents frequency instead of wavenumber, and the asterisk on ν is dropped for convenience, but with the implicit assumption that the integration over the finite bandpass (which is usually very narrow in the microwave region and is assumed to be rectangular) has already been accomplished. Also, microwave radiometers usually are calibrated in terms of brightness temperature measurements T_b instead of radiance, since radiance is a linear function of temperature in the microwave region.

Once these changes are incorporated, the form of upward-propagating radiation $T_u(\nu,\theta)$ is analogous to eq. (3) except for the explicit spectral emissivity factor $\varepsilon(\nu,\theta)$ in the boundary term, that is,

$$T_u(\nu,\theta) = \varepsilon(\nu,\theta)\ T(x_s)\ \ \bar{\tau}(\nu,\theta,x_s) + \int_0^{x_s} T(x)\left(-\frac{d\bar{\tau}(\nu,\theta,x)}{dx}\right) dx. \tag{10}$$

Since $\varepsilon(\nu,\theta)$ is less than unity, there must be a reflected component, with reflectivity $\rho(\nu,\theta) = 1-\varepsilon(\nu,\theta)$. If we assume specular reflection, this reflected component is a product of three factors: The first is the downward-propagating component $T_d(\nu,\theta)$, namely,

$$T_d(\nu,\theta) = \int_0^{x_s} T(x)\ \left(\frac{d\bar{\tau}(\nu,\theta,x,x_s)}{dx}\right) dx + \bar{\tau}(\nu,\theta,0,x_s)\ T_{sp}, \tag{11}$$

where $\bar{\tau}(\nu,\theta,x,x_s)$ is the mean transmittance from the atmospheric level x to the surface x_s, and T_{sp} = 2.96K is the temperature of cold space above x=0, the effective top of the atmosphere. The second factor is the reflectivity $\rho(\nu,\theta)$ itself, and the third is the surface transmittance $\bar{\tau}(\nu,\theta,x_s)$. Therefore, the brightness temperature measured by the microwave radiometer is

$$T_b(\nu,\theta) = T_u(\nu,\theta) + \rho(\nu,\theta)\quad \bar{\tau}(\nu,\theta,x_s)\ T_d(\nu,\theta). \tag{12}$$

By combining eqs. (11) and (12), one sees that the contribution from space is $\rho(\nu,\theta)\,\bar{\tau}(\nu,\theta,x_s)\,\bar{\tau}(\nu,\theta,0,x_s)T_{sp}$. Since this quantity is very small (or even zero for the more opaque channels), it is ignored. Also ignored are polarization effects from the reflection at the surface.

Equation (11) requires downward-propagating transmittances $\tau(\nu,\theta,x,x_s)$, but the TOVS software system provides only upward-propagating transmittances $\tau(\nu,\theta,x) = \tau(\nu,\theta,x,0)$. This difficulty is resolved by the identity

$$\tau(\nu,\theta,x,x_s) = \tau(\nu,\theta,x_s,0)/\tau(\nu,\theta,x,0) = \tau(\nu,\theta,x_s)/\ \tau(\nu,\theta,x), \tag{13}$$

which follows from the definition for monochromatic transmittance,

$$\tau(\nu,\theta,x_2,x_1) = \tau(\nu,\theta,x_1,x_2) = \exp\ [-(q\ \sec\theta/g) \int_{P(x_1)}^{P(x_2)} k(\nu,T,p)dp], \tag{14}$$

where by definition

$$P(x_2) \geq P(x_1),$$

and where q is the constant mass mixing ratio of molecular oxygen, g is acceleration of gravity, and k is the absorption coefficient. There is an additional problem in that the transmittances available for use in eq. (13) are not monochromatic. As indicated previously, they have been integrated over a rectangular band-pass function. However, eq. (13) appears to be sufficiently accurate, because (1) the response function is narrow and is essentially symmetric about its centroid, and (2) as shown in fig. 7, the O_2 transmittance in the microwave region arises from the "valleys" between pairs of spectral lines where the transmittance varies relatively slowly with frequency.

When eqs. (10), (11), and (13) are inserted into eq. (12), one obtains

$$T_b(\nu,\theta) = \varepsilon(\nu,\theta)\ T(x_s)\ \bar{\tau}(\nu,\theta,x_s) + \int_0^{x_s} T(x)\ (-\frac{d\tilde{\tau}(\nu,\theta,x)}{dx})\ dx, \tag{15}$$

where

$$\frac{d\tilde{\tau}(\nu,\theta,x)}{dx} = \left\{ 1 + [1-\varepsilon(\nu,\theta)] \left[\frac{\bar{\tau}(\nu,\theta,x_s)}{\bar{\tau}(\nu,\theta,x)}\right]^2 \right\} \frac{d\bar{\tau}(\nu,\theta,x)}{dx} \tag{16}$$

We call $d\tilde{\tau}/dx$ the "effective" mean weighting function. Notice that eq. (15) is directly analogous to the infrared form of the radiative transfer equation, namely eq. (3). Furthermore, by integrating eq. (16), one obtains the "effective" mean transmittance function,

$$\tilde{\tau}(\nu,\theta,x) = \left\{ 1 - [1-\varepsilon(\nu,\theta)] \left[\frac{\bar{\tau}(\nu,\theta,x_s)}{\bar{\tau}(\nu,\theta,x)}\right]^2 \right\} \bar{\tau}(\nu,\theta,x). \tag{17}$$

This is the form actually used in the TOVS processing system to compute the transmittance functions. The derivatives are computed not by eq. (16), but by difference quotients applied to eq. (17). Thereupon the brightness temperatures are obtained from eq. (15).

If one considers a channel where the atmosphere is opaque, then $\bar{\tau}(\nu,\theta,x_s)$ is very small, and eqs. (15) and (16) reduce to

$$T_b(\nu,\theta) = \int_0^{x_s} T(x) \left(- \frac{d\bar{\tau}(\nu,\theta,x)}{dx}\right) dx = T_u(\nu,\theta), \tag{18}$$

in agreement with eq. (12) in the limit as $\bar{\tau}(\nu,\theta,x_s)$ approaches zero.

As mentioned in the Introduction, the TOVS operational retrieval procedure is a regression procedure. However, if one wished to solve the radiative transfer equation as an integral equation, he would start with eq. (15).

Although eqs. (15) - (18) are what are needed to calculate T_b operationally, their derivation nevertheless involves some approximation in that eq. (13) is assumed to hold for polychromatic radiation. One can derive an alternative equation for T_b that involves no approximation. Starting with eqs. (10), (11) and (13) in their monochromatic form (i.e., with $\bar{\tau}$ replaced by τ), and inserting them into the monochromatic form of eq. (12), one obtains monochromatic forms of eqs. (15) and (16), which involve no approximations. Then, if the monochromatic form of eq. (15) is multiplied by the rectangular instrument response function $\hat{\phi}(\nu,\nu^*)$ and integrated over the bandpass from ν_1 to ν_2, and if the order of integration is interchanged, one obtains

$$T_b(\nu,\theta) = T(x_s)\, \bar{\tau}(\nu^*,\theta,x_s) + \int_0^{x_s} T(x) \left(- \frac{d\bar{\tilde{\tau}}(\nu^*,\theta,x)}{dx}\right) dx, \tag{19}$$

where

$$\bar{\tau}(\nu^*,\theta,x_s) = \int_{\nu_1'}^{\nu_2} \hat{\phi}(\nu,\nu^*)\ \varepsilon(\nu,\theta)\ \ \tau(\nu,\theta,x_s)\, d\nu \tag{20}$$

is the mean transmittance in analogy with eq. (4), and

$$\frac{d\bar{\tilde{\tau}}(\nu^*,\theta,x)}{dx} = \int_{\nu_1}^{\nu_2} \hat{\phi}(\nu,\nu^*)\ \frac{d\tilde{\tau}(\nu,\theta,x)}{dx}\, d\nu = \frac{d}{dx}\int_{\nu_1}^{\nu_2} \hat{\phi}(\nu,\nu^*)\ \tilde{\tau}(\nu,\theta,x)\, d\nu \tag{21}$$

is the derivative of the mean transmittance in analogy with eq. (6). Note that since eqs. (15) and (19) involve T(x), which unlike the Planck function is independent of ν, the mean-value theorem is not required, and, therefore, the concept of the effective temperature developed in Section 2.2.1 is not needed for microwave retrievals.

2.3 Treatment of Transmittances in the Multigas Atmosphere

2.3.1 Infrared Region

Of the twenty HIRS channels, eighteen are used for sounding atmospheric temperature and water vapor, and these are the ones for which we calculate transmittances. (No transmittances are produced for channels 9 and 20.) The atmospheric gases that absorb significantly in vertical and slant paths in the spectral intervals of the HIRS are CO_2, N_2O, CO, CH_4, H_2O, O_3, and N_2. We ignore extinction by aerosols, following Stowe (1974) and Stowe and Fleming (1980).

Carbon dioxide is treated as uniformly mixed (330 ppmV) in the atmosphere. Following McClatchey et al. (1973), we also treat N_2O (0.28 ppmV), CO (0.075 ppmV), and CH_4 (1.6 ppmV) as uniformly mixed. This is an adequate approximation for CO and CH_4, mainly because they are relatively unimportant as absorbers in the HIRS intervals. However, for N_2O, which is a major absorber in channels near 4.3 µm, this treatment may be too crude. The mixing ratio of N_2O decreases with increasing altitude in the upper troposphere and the stratosphere (Banks and Kockarts 1973) and probably varies diurnally (Matthias et al. 1979). Incidentally, the average tropospheric mixing ratio of N_2O was recently found to be about 0.33 ppmV (Cicerone et al. 1978), which exceeds the older value of 0.28 ppmV that McClatchey et al. (1973) quote and that we use. Molecular nitrogen, which has a broad collision-induced band near 4.3 µm, is justifiably treated as uniformly mixed. On the other hand, water vapor and ozone, which are important absorbers, do have their variability taken into account.

Figures 1-5 show the spectral intervals of HIRS idealized as triangles and accompanied by spectra of atmospheric constituents. Figure 1 shows the positions of channels 1-7 in relation to the lines in the 15-µm band of CO_2. Figure 2 shows channels 13-17 with lines of both the 4.3-µm band of CO_2 and the ν_3 band of N_2O. Figure 3 shows channels 10-12 with lines of the ν_2 water-vapor band centered near 6.3 µm. Figure 4 shows channel 8, which is in the 11-µm window, a region of weak water-vapor lines. The water-vapor continuum causes the envelope of the spectrum to have a transmittance of approximately .98 rather than 1. Incidentally, this spectrum was measured in a relatively dry atmosphere (total water = 0.6 g/cm^2), where the water-vapor absorption is comparatively weak. With a more humid atmosphere the absorption will be stronger. Figure 5 shows channels 18 and 19 in the 3.8-μm window, with weak absorption dominated by N_2O near 2570 cm^{-1} and by HDO and CH_4 betweem 2700 and 2850 cm^{-1}. The strong absorption at wavenumbers less than 2500 cm^{-1} is due to unresolved lines of N_2O and CO_2 and the nitrogen collision-induced feature centered at 2330 cm^{-1}.

In most spectral intervals of the HIRS, more than one gas has to be included in the computation of atmospheric transmittance. For computational convenience we treat the atmospheric absorption as originating from the following six sources:

1. Spectral lines of the uniformly-mixed gases (CO_2, N_2O, CH_4, CO, O_2),
2. Spectral lines of water vapor,
3. Spectral lines of ozone,
4. Water-vapor self-broadened continuum,
5. Water-vapor foreign-broadened continuum, and
6. Collision-induced band of molecular nitrogen.

The transmittance of the atmosphere is formed as the product of the transmittances of these constituents (Goody 1964).

In the preceding list, the first source combines absorption by five of the gases treated as uniformly mixed. We synthesize a single transmittance for this multi-gas source in the line-by-line calculations, which we perform in advance off line to produce coefficients for the on-line "rapid" algorithm (see Section 3). These line-by-line calculations involve all five gases simultaneously and account for the overlap among lines of different gases, with the result that a single set of coefficients is produced for application in a single on-line algorithm. On the other hand, a single gas, water vapor, contributes absorption from three sources -- spectral lines, foreign-broadened continuum, and self-broadened continuum (see, e.g., Roberts, Selby, and Biberman 1976).

Table 4 shows, for each channel of the HIRS, which sources contribute in the calculation of transmittance. An M in the table signifies that the absorber is the main one for that channel, whereas an I signifies a less important, but non-negligible, interfering absorption. The criterion for an absorber to be included in the calculation is that it must decrease the atmospheric transmittance by at least 0.005 at at least one level in the atmosphere. We derived table 4 by applying this criterion to profiles of transmittances that had been calculated as follows[2]: For spectral lines of the uniformly-mixed gases and water vapor, we used line-by-line calculations (Arking 1977, Neuendorffer 1977; also see section 3.3.1). Absorption by the

---

[2]These procedures differ slightly from those to be described in section 3, because this work was done earlier and with the sole purpose of choosing constituents to include in the operational calculation.

two water vapor continua and by nitrogen was computed as described in sections 4.2 and 4.3. Ozone was treated less rigorously. Its role was determined from calculations done earlier for the Vertical Temperature Profile Radiometer (McMillin et al. 1973) and from spectra in the Migeotte atlas (1957). This atlas was also used to check qualitatively the results of many of the other calculations described above. Measurements of atmospheric transmittances in window regions (Weinreb et al. 1977) were used to verify the results in channels 8, 18, and 19.

Table 4.--Contributors in transmittance calculations for infrared channels

CHANNEL	CENTRAL WAVE NO. (cm^{-1})	SPECTRAL LINES OF UNIFORMLY MIXED GASES	H_2O LINES	OZONE LINES	CONTINUA H_2O SELF	CONTINUA H_2O FOREIGN	N_2
HIRS 1	668	M		I			
HIRS 2	679	M		I			
HIRS 3	691	M		I			
HIRS 4	704	M	I	I	I		
HIRS 5	716	M	I	I	I		
HIRS 6	732	M	I	I	I		
HIRS 7	748	M	I	I	I		
HIRS 8	898		I		I		
HIRS 9	1028						
HIRS 10	1217	I	M		M	M	
HIRS 11	1364	I	M		M	M	
HIRS 12	1484		M		M	M	
HIRS 13	2190	M	I		I	I	I
HIRS 14	2213	M	I		I	I	I
HIRS 15	2240	M	I		I	I	I
HIRS 16	2276	M					
HIRS 17	2361	M					
HIRS 18	2513	I	I		I	I	I
HIRS 19	2671	I	I		I	I	
SSU 1	665	M					
SSU 2	665	M					
SSU 3	665	M					

Table 4 shows that the absorption in HIRS channels 1-7 is dominated by the uniformly-mixed gases, specifically by the 15-μm band of CO_2, but ozone, water-vapor lines, and the self-broadened continuum also contribute. Channels 10-12 of HIRS sense mainly water vapor but are also affected by the uniformly-mixed gases, chiefly methane. Absorption in channels 13-17 of HIRS is dominated by the uniformly mixed gases, principally the 4.5-μm band of N_2O and the 4.3-μm band of CO_2, with some interfering absorption by molecular nitrogen and the three water-vapor constituents. The HIRS channels 8, 18, and 19 are atmospheric "window" channels, which are intended for sensing the earth's surface, and where any absorption is considered to be interference. In channels 8 and 19 water vapor is the principal absorber, while in channel 18 both nitrogen and water vapor are important. The contribution of the uniformly-mixed gases in channels 18 and 19 is relatively unimportant.

Transmittances are also calculated for the three channels of the SSU. The pressure modulating in these channels restricts the atmospheric absorption to that by carbon dioxide alone, and the filter further restricts it to the 15-μm band. This is indicated in the last three rows of table 4.

2.3.2 Microwave Region

Figure 6 shows the microwave spectrum of O_2 and H_2O under low resolution. The channels of the MSU are located in the 50-60 GHz region, where a strong rotational oxygen band dominates the absorption. Overlapping this absorption is a weak non-resonant absorption by water vapor, due principally to the wings of the lines centered near 22 and 183 GHz. A high-resolution O_2 spectrum appears in fig. 7. It shows that the O_2 absorption near 60 GHz arises from a series of lines spaced roughly every 500 MHz. The line widths vary with altitude from roughly 700 MHz at 1000 mb to 20 MHz at 10 mb. Also shown in fig. 7 are schematic representations of the passbands of channels 2 and 3 of the MSU, which are fitted into the regions between the oxygen lines, where the atmospheric absorption varies slowly with frequency.

3. ALGORITHMS FOR SPECTRAL LINES IN THE INFRARED

3.1 General Approach

As Section 2.3 explained, atmospheric transmittances in the infrared are computed in the TOVS processing system as products of transmittances from up to six sources (see table 4). The remainder of this report presents our methods of calculating transmittances for each source. The following two sections (3.2 and 3.3) treat the contribution by spectral lines of the uniformly-mixed gases and of water vapor. Line transmittances are most accurately calculated by the line-by-line method. However, calculations with this method consume so much time that they cannot be done on line. It is estimated that for a single temperature retrieval by a non-regression (physical) method of solution, the required transmittance calculations, if done line by line, would take about ten minutes on the IBM 360/195 at NOAA. At this rate, processing of a two-hour orbit would tie up the computer for one week! The approximation techniques used operationally are described in section 3.2, while section 3.3 describes the off-line work, which includes line-by-line calculations, to prepare the coefficients needed in the approximations.

The variables and the coordinate system for the transmittance calculations are as follows: As shown in fig. 8, the atmosphere is represented by a series of 39 parallel, homogeneous layers that are bounded by the 40 atmospheric levels defined in table 5. At these levels values are prescribed for pressure P(mb), temperature T(K), and water-vapor mixing ratio q (g/Kg). The zenith angle θ, shown in fig. 8, is the angle between the line of sight and the local vertical. For a given channel and zenith angle, transmittances are calculated for 40 paths. Each path originates at the satellite and terminates at one of the 40 atmospheric levels. For a path terminating at level i, with zenith angle θ, and for a channel whose central wavenumber is ν, the transmittance is denoted by $\tau(\nu,\theta,i)$. Of course, it should be understood that the transmittance also depends on properties of the atmosphere (e.g., P, T, q) that for convenience are not included in the list of arguments. Note also that unless we specify otherwise, the symbol τ and the term "transmittance" henceforth refer to spectral averages as defined in eq. (4).

Table 5.--The 40 levels for atmospheric computations

Level	Pressure (mb)	Level	Pressure (mb)	Level	Pressure (mb)	Level	Pressure (mb)
1	0.1	11	10	21	115	31	500
2	0.2	12	15	22	135	32	570
3	0.5	13	20	23	150	33	620
4	1.0	14	25	24	200	34	670
5	1.5	15	30	25	250	35	700
6	2.0	16	50	26	300	36	780
7	3.0	17	60	27	350	37	850
8	4.0	18	70	28	400	38	920
9	5.0	19	85	29	430	39	950
10	7.0	20	100	30	475	40	1000

3.2 Description of Algorithms (On Line)

3.2.1 Uniformly-Mixed Gases

In this section a fast and accurate approximation for computing polychromatic transmittances in inhomogeneous atmospheres for the uniformly-mixed gases (CO_2, N_2O, CH_4, O_2 and CO) is discussed. This algorithm is applied in 16 of the HIRS channels and in all three SSU channels. Because the procedure is described in a series of published papers, only an outline of the method is presented here. For details the reader should consult the original papers--McMillin and Fleming (1976) and Fleming and McMillin (1977).

The algorithm is a recurrence procedure in which the transmittance $\tau(\nu,0,i)$ for central wavenumber ν, zero zenith angle, the ith atmospheric level, and an arbitrary temperature profile T, is given by

$$\tau(\nu,0,i) = \tau(\nu,0,i-1)\,[\alpha_i(\nu) + \beta_i(\nu)\Delta T_i + \delta_i(\nu)\Delta T_i^2 + \zeta_i(\nu)\Delta T^*_i + \eta_i(\nu)\,\Delta T^{**}_i], \qquad i=1,\ldots,40; \tag{22}$$

with $\tau(\nu,0,0) = 1.0$. In eq. (22) the coefficients are determined by an ordinary least squares procedure as described below in section 3.3.2; $\Delta T_i = T_i - \hat{T}_i$ is the deviation of the given temperature T at level i from a given reference profile $\hat{T}$ at level i; and the effective temperature deviations are given by

$$\Delta T_i^* = \frac{1}{P_i} \sum_{j=1}^{i} \Delta T_j \, \Delta P_j = (P_{i-1} \, \Delta T_{i-1}^* + \Delta T_i \, \Delta P_i)/P_i \qquad (23)$$

and

$$\Delta T_i^{**} = \frac{2}{P_i^2} \sum_{j=1}^{i} P_j \Delta T_j \Delta P_j = (P_{i-1}^2 \, \Delta T_{i-1}^{**} + 2P_i \Delta T_i \Delta P_i)/P_i^2, \qquad (24)$$

where $\Delta P_j = P_j - P_{j-1}$ with $P_0 = 0$.

The theoretical and numerical basis for the general form of eq. (22) is developed in McMillin and Fleming (1976), sections II and III. Effective temperatures ΔT^* and ΔT^{**} serve as adjustment terms that extend the validity of eq. (22) from monochromatic to polychromatic transmittances. Justification for the use of the effective temperatures for this purpose is given in McMillin et al. (1979), section IV.

A second algorithm is required to calculate the polychromatic transmittance for an arbitrary zenith angle θ. This is easily accomplished by the approach of eq. (22), which results in an algorithm of the form

$$\tau(\nu,\theta,i) = \tau(\nu,0,i) + (\sec\theta - 1)\,[a_i(\nu) + b_i(\nu)\Delta T_i^{**} + c_i(\nu)(\sec\theta - 1)], \qquad (25)$$

$$i = 1,\ldots,40;$$

where $\tau(\nu, 0, i)$ is obtained directly from algorithm (22), ΔT_i^{**} is given by eq. (24), and the computation of the coefficients is by least squares, as described in section 3.3.2.

The accuracy of algorithms (22) and (25) is consistent with the present-day accuracy of the spectroscopic parameters that are used in the line-by-line computer programs that calculate atmospheric transmittances. Specific accuracy statements are given in each of the three papers cited at the beginning of this section and in McMillin et al. (1980).

The implementation of algorithm (22) is quite straightforward. One starts with knowledge of all 5x40 coefficients and the actual and reference temperatures given at 40 discrete pressure levels. Then i is set equal to 1, and $\tau(1)$ is calculated using $\tau(0) = 1$. With $\tau(1)$ in hand, one next calculates $\tau(2)$, and so on, recurrently, until the transmittance at the ground $\tau(40)$ is obtained. Clearly, each $\tau(k)$ depends functionally on the temperature profile and all the transmittances above the level k (i.e., on all $i < k$), as we know happens physically in the real atmosphere. Note that when $T = \hat{T}$, the algorithm reduces to $\tau(i) = \tau(i-1)\alpha_i$, which is to say that α_i is just the ratio of $\tau(i)$ to $\tau(i-1)$ for the reference temperature profile.

For a nonzero zenith angle, the τ's obtained from algorithm (22) are used in algorithm (25), along with the 3x40 known coefficients, the secant of the angle θ, and ΔT_i^{**} calculated from eq. (24) for the same two temperature profiles as used in algorithm (22). Note that this algorithm is not recurrent, but simply an adjustment to the zero zenith angle case.

3.2.2 Spectral Lines of Water Vapor

We apply the method of Weinreb and Neuendorffer (1973) to calculate polychromatic atmospheric transmittances associated with spectral lines of water vapor. The quantity of water vapor U_i between the satellite and the i th level is calculated from the mixing ratios q by the summation,

$$U_i = \frac{\sec\theta}{2g} \sum_{j=2}^{i} (q_j + q_{j-1})\,(P_j - P_{j-1}), \quad i=2, \tag{26}$$

where $g = 980.665 \text{ cm sec}^{-2}$, and where $U_1 = 0$ (i.e., there is no water vapor between the satellite and level 1). The absorber amount ΔU_i in the i th layer, which is bounded by levels i-1 and i, is given by

$$\Delta U_i = U_i - U_{i-1} \,. \tag{27}$$

Also, for pressure and temperature in the i th layer we assign the mean values $\bar{P}_i$ and $\bar{T}_i$, where

$$\bar{P}_i = (P_i + P_{i-1})/2,$$

$$\bar{T}_i = (T_i + T_{i-1})/2.$$

Note that the quantities on the right sides of these equations, P and T, are prescribed at levels, whereas $\bar{P}$ and $\bar{T}$ are assigned to represent the conditions for the entire layer. (For the relationship between layers and levels, see fig. 8).

For each channel, transmittances are to be computed for the paths between the satellite and each of the 40 levels. For the channel with central wavenumber ν we define $\tau(\nu,\theta,i)$ to be the transmittance to level i along the slant path specified by θ. The effect of zenith angle is completely accounted for in the computation of U (eq. 26). In all other respects the computations of transmittance are identical for all θ. To simplify the notation we henceforth suppress the reference to θ and ν, and $\tau(i)$ represents the transmittance to level i.

It is assumed that a model is given for computing transmittances in homogeneous paths. (A homogeneous path is a path characterized by a single fixed set of conditions--pressure, temperature, and water-vapor mixing ratio, as in a laboratory cell.) The model is presented below. First, however, we describe the application of such a model to an inhomogeneous atmosphere. Let the model be represented by

$$\tau = f(P,T,U).$$

To start, since we assumed $U_1 = 0$, the transmittance through the layer between the satellite and level 1 will be given by $\tau(1) = 1$. The transmittance $\tau(2)$ at the bottom of the second layer is computed from the model under the conditions in layer 2 -- $\overline{P}_2$, $\overline{T}_2$, and U_2; i.e.,

$$\tau(2) = f(\overline{P}_2, \overline{T}_2, U_2).$$

The method now works downward through the remaining levels of the atmosphere, as follows: Given $\tau(i-1)$, we first calculate the value of U that would produce this value with the conditions of pressure and temperature in the next layer (i); i.e., if we let V_i be the required value of U, it satisfies the equation,

$$\tau(i-1) = f(\overline{P}_i, \overline{T}_i, V_i) . \qquad (28)$$

This equation can be inverted by Newton's method to determine V_i. Next, we calculate a new "effective" amount of water vapor W_i between the satellite and level i by adding to V_i the known amount of water vapor ΔU_i in layer i,

$$W_i = V_i + \Delta U_i.$$

Finally, we produce $\tau(i)$, the transmittance at the bottom of layer i, by evaluating the model for W_i and the conditions in layer i; i.e.,

$$\tau(i) = f \ (\overline{P}_i, \overline{T}_i, W_i).$$

It is seen that this method operates by scaling the water-vapor amount U. Because of eq. (28), the scaled value W_i depends explicitly on the conditions in layer i and implicitly, through $\tau(i-1)$, on the conditions in the layers above.

It remains to present the model $f(P,T,U)$. Following Smith (1969), we use a polynomial expansion (strictly speaking, not really a model),

$$\ln(-\ln \tau) = \sum_{j=1}^{14} C_j(\nu)\, X_j\ , \tag{29}$$

where

$X_1 = 1$, $X_2 = 0.1 \ln(UT/273)$, $X_3 = \ln(P/1000)$,

$X_4 = \ln(T/273)$, $X_5 = X_2X_3$, $X_6 = X_2X_4$,

$X_7 = X_2^2$, $X_8 = X_4X_7$, $X_9 = X_3X_4$,

$X_{10} = X_2X_7$, $X_{11} = X_4X_6$, $X_{12} = X_4^2$,

$X_{13} = X_3X_6$, and $X_{14} = X_3X_7$.

The coefficients C_j are dependent on channel ν. For each channel, the C_j were derived off-line from a least-squares fitting of the polynomial to transmittances calculated line-by-line and convoluted with the spectral response function for a large dependent sample of homogeneous paths, as described in section 3.3.

The accuracy of this algorithm, described in the publication cited above, is more than sufficient for this application. In fact, the largest errors incurred in calculating transmittances for water vapor are not caused by deficiencies in the technique of the calculation, but rather by our poor knowledge of the mixing ratio of water vapor in the troposphere (Weinreb 1977).

3.3 Generation of Coefficients (Off Line)

3.3.1 Line-by-line Technique

We evaluate the coefficients for the approximations presented in the preceding two sections by fitting each approximation to a set of transmittances calculated line by line. This section summarizes how line-by-line calculations are done at NESS. Subsequent sections describe how they are applied in generating the coefficients.

Our line-by-line algorithm was developed by Neuendorffer (1977) to minimize computation time without sacrificing accuracy or flexibility. Transmittances are produced at a resolution of 0.1 cm^{-1}, but the internal computations are done at a resolution of 0.02 cm^{-1}. Even the latter resolution is inadequate to treat absorption near centers of the very narrow lines encountered at the lowest atmospheric pressures. The centers of such spectral lines are assumed to be described by Voigt functions, which we treat by single-line modelling. The modelling is done only in the region of the spectrum within 0.02 cm^{-1} of the centers of spectral lines whose widths are less than 0.006 cm^{-1}. Such linewidths occur at atmospheric pressures below approximately 100 mb. Outside the regions that are modelled, the absorption coefficient is constructed as a linear combination of four Lorentz functions characterized by their (four) values of halfwidth. The Lorentz functions are generated as convolutions, which are accomplished efficiently via fast Fourier transforms.

In applying this line-by-line technique to produce transmittances for HIRS, we used line parameters from the 1976 version of the AGFL tape of line parameters (McClatchey et al. 1973, Rothman and McClatchey 1976). We also made the following physical assumptions:

a. Lorentz halfwidths are proportional to $T^{-0.5}$.

b. The formulation of line strengths follows McClatchey et al. (1973) and does not include a factor for simulated emission.

c. Linewings terminate at 11 cm^{-1} from line centers.

d. For the uniformly mixed gases (but not for water vapor), line profiles are computed as products of Lorentz profiles and a function $\chi(\nu-\nu o)$ (Winters et al. 1964, Burch et al. 1969, Susskind and Searl 1978), where

$$\chi(\nu-\nu_o) = \left(1 + \frac{2|\nu-\nu_o|}{a}\right) \exp\left(-\frac{2|\nu-\nu_o|}{a}\right),$$

ν_o = wavenumber at line center,
and $a = 11\ cm^{-1}$.

This function reduces absorption in linewings and brings calculated transmittances into accord with measurements, as described in the previously cited references.

e. Mixing ratios of atmospheric gases are as given in section 2.3.1.

3.3.2 Coefficients for Uniformly-Mixed Gases

a. HIRS Channels

Coefficients for eqs. (22) and (25) are produced as described in McMillin and Fleming (1976) and Fleming and McMillin (1977), resp. The procedures are based on transmittances generated line by line at a resolution of 0.1 cm^{-1}, as explained in the previous section, for the range of the infrared spectrum spanned by the HIRS channels (600-1380 cm^{-1} and 2100-3060 cm^{-1}). Transmittances are calculated for the following conditions:

1. The 40 atmospheric levels listed in table 5.

2. The 19 temperature profiles listed in Appendix A.

3. Five zenith angles: $\sec\theta = 1, 5/4, 6/4, 7/4, 2$.

Since these transmittances are independent of any instrument's characteristics, they are computed once and for all and are stored on disk as an array with 17,400 (spectral points) x 40 (levels) x 19 (profiles) x 5 (angles) elements.

Once the spectral response functions of a particular HIRS instrument become known, we compute the coefficients as follows: First the 0.1 cm^{-1}-resolution transmittances are convoluted with the spectral response functions for the 19 channels listed in table 4. This yields a 19 (channels) x 40 x 19 x 5-element array of mean transmittances. These are the quantities used in the radiative transfer equation as defined in eq. (4). Henceforth we omit the modifier "mean" and refer to them simply as transmittances. In deriving coefficients for eq. (22), we work only with transmittances calculated at zero zenith. Furthermore, we use only the transmittances generated for the first 16 of the 19 temperature profiles, deferring use of the remaining three profiles to test the accuracy of eq. (22). Hence, for each combination of channel and level, there are available 16 sets of transmittances and their associated values of the predictors ΔT, ΔT^*, and ΔT^{**}. These are used in a least-squares procedure to evaluate the coefficients for eq. (22).

We check the validity of the coefficients by applying eq. (22) in calculating transmittances for the remaining three temperature profiles in Appendix A. "Correct" transmittances have already been generated as described previously, via line-by-line calculations and convolutions with the instrument response functions. The "errors" in the transmittances from eq. (22) are less than 0.002 for most channels and levels when the procedures are working satisfactorily.

Coefficients for eq. (25) are generated by procedures described in Fleming and McMillin (1977). We utilize transmittances calculated for five zenith angles to form "deviations" from zero zenith, $\tau(\nu,\theta,i) - \tau(\nu,0,i)$. For each combination of channel and level, there are available 16 (profiles) x 4 (zenith deviations) sets of deviations and their associated values of the predictors ΔT^{**} and $(\sec\theta - 1)$. These are used in a least-squares procedure to evaluate the coefficients in eq. (25). The validity of these coefficients is similarly tested on the transmittances for the three remaining temperature profiles.

b. SSU Channels

Coefficients for eqs. (22) and (25) are evaluated for the SSU channels by procedures similar to those for the HIRS channels, but with two differences. The first is rather minor: Calculations are done not for the five zenith angles listed previously, but for five nadir angles--0°, 5°, 15°, 25°, and 35°. (The latter four angles are the nominal scan positions of the SSU.) The second difference is in the line-by-line algorithm. For the SSU , the line-by-line computations are done by Dr. David Pick (1980) of the British Meteorological Office. They are based on the program originally described by Drayson (1966), and they use line parameters from the AFGL tape (McClatchey et al. 1973). For each of the 19 temperature profiles, transmittances are computed at 0.1-cm^{-1} resolution for radiation traversing the atmosphere and the CO_2 in the 1 cm^{-1}-long SSU cell. The computations are done twice, once for the highest and once for the lowest pressures achieved in the cell during modulation. The theoretical SSU transmittances result when one convolutes the difference between the two computations with the SSU's filter response functions. Finally, empirical adjustments are applied to the theoretical transmittances, based on measurements made with the SSU in the laboratory. The line-by-line calculations are done twice--for a cell having the nominal value of mean pressure, and for a cell having a mean pressure that is 10 percent higher. The two resulting arrays of transmittances, each 3 (channels) x 40 (levels) x 19 (profiles) x 5 (angles) in size, are then given to NESS.

Shortly before launch of the TOVS, the British Meteorological Office provides NESS with the "effective" mean cell pressure, which it has determined by requiring agreement in the 0.5-transmittance region between calculated transmittances and those obtained in the laboratory. (After launch, it is planned that the British Meteorlogical Office occasionally provide NESS with revised effective mean cell pressures that are determined from comparisons between radiance measurements and integrated rocketsonde profiles.) At NESS, we interpolate the transmittances to the effective mean cell pressure, using the two arrays of transmittances provided by the British. The coefficients for eqs. (22) and (25) are then determined and checked by the procedures described in part (a) of this section.

3.3.3 Coefficients for Spectral Lines of Water Vapor

Coefficients for eq. (29) are determined from a set of transmittances computed line by line for 144 homogeneous paths in water vapor-air mixtures. (Recall that a homogeneous path is one in which the temperature, pressure, and water-vapor mixing ratio each have a single value, as in a laboratory cell.) The conditions defining the 144 paths are listed in Appendix B. Transmittances are generated line by line at a resolution of 0.1 cm^{-1} for the spectral range of 270-1650 cm^{-1} and 2100-3060 cm^{-1}, yielding a 23400 (spectral points) x 144 (paths) array. These transmittances are independent of any instrument's characteristics and are computed once and for all and stored on disk. Once the characteristics of a given HIRS instrument are known, the transmittances are convoluted with the spectral response functions in the 13 channels that experience water vapor absorption (see table 4), producing a 13 (channel) x 144-element array of (mean) transmittances. For each channel, we fit eq. (29) by least squares to the 144 transmittances and their associated values of P, T, and U, thereby evaluating the coefficients C_i, i=1,..., 14.

4. OTHER ALGORITHMS IN THE INFRARED

4.1 Ozone

There is an ozone absorption band at 14 μm that overlaps the 15-μm CO_2 band. Even though this ozone band is weak, it cannot be ignored, because it can affect the absorption in the 690-cm^{-1} channel by as much as 10 percent. On the other hand, the band's weakness allows us to make simplifications in the algorithm used to account for its absorption.

As table 4, shows, we compute ozone transmittances only in channels 1-7. We do not compute transmittances operationally for channel 9. Although channel 9 is spectrally located near the center of ozone's 9.6-μm absorption band and is used in operational retrievals of total ozone amounts, the retrieval is by regression, and transmittances are not involved.

Briefly, the scheme is a linear interpolation, based on total ozone amount, between two transmittance profiles (transmittance vs atmospheric level) corresponding to opposing extreme distributions of ozone. The two transmittance profiles were calculated line by line (Kunde and Maguire 1974) for specific ozone concentration profiles having total ozone amounts of 257 and 480 Dobson units (one Dobson unit equals 10^{-3} cm of ozone at NTP). The two concentration profiles were assumed to be typical for these two extreme total ozone amounts. The line-by-line calculations of transmittance, averaged over 0.1-cm^{-1} intervals (see Section 3.3.1 for details of similar calculations), were convoluted with the instrument response function. We will refer to the resulting two transmittance profiles henceforth as τ_{257} (ν,0,i) and τ_{480} (ν,0,i), where ν is the wavenumber corresponding to the response function centroid for the channel, the zero refers to the zero zenith angle, and i is the index corresponding to atmospheric pressure (see table 5).

With the profiles τ_{257} and τ_{480} in hand, one needs only the total ozone amount corresponding to the geographical location at which the transmittance curve is required. The total ozone amount Ω is computed simultaneously with the other operational sounding products. However, if this estimate is not available to a user, Ω can be computed from climatological data of fig. 9. For purposes of automatic computation on a computer one can either fit the four curves in fig. 9 by closed-form algebraic expressions, such as polynomials, or set up a table of values extracted from the figure. If a finer breakdown of the data than by season is required, one can interpolate between the closed-form expressions or interpolate among the tabular values, as the case may be. Also, even though it is not really correct, the winter curve of fig. 9 is used as the Southern Hemisphere summer curve, and so forth. For a more detailed and up-to-date graph of the distribution of ozone by season and latitude (including the Southern Hemisphere) see London (1978).

The linear interpolation formula that yields the estimate of the transmittance profile at zero zenith angle is given by

$$\tau(\nu,0,i) = (1-\alpha)\tau_{257}(\nu,0,i) + \alpha\,\tau_{480}(\nu,0,i), \tag{30}$$

where the interpolation parameter α is obtained from the ratio

$$\alpha = \frac{\Omega - 257}{480-257} = 0.00448\,\Omega - 1.152. \tag{31}$$

Note that for ozone amounts outside the range 257 to 480 Dobson units, eq. (30) represents an extrapolation.

Equation (30) must be generalized for transmittances calculated at nonzero zenith angles. It was found that the following form yielded satisfactory results:

$$\tau(\nu,\theta,i) = (1-\alpha)\left[\tau_{257}(\nu,0,i)\right]^{1+a_\nu(i)(\sec\theta-1)} + \alpha\left[\tau_{480}(\nu,0,i)\right]^{1+b_\nu(i)(\sec\theta-1)}. \tag{32}$$

The coefficients a and b in eq. (32) are determined from two special values of τ in eq. (32), namely, $\tau = \tau_{257}(\nu, 60^\circ, i)$ and $\tau = \tau_{480}(\nu, 60^\circ, i)$, which yield the results

$$a_\nu(i) = \frac{\ln\tau_{257}(\nu,60^\circ,i)}{\ln\tau_{257}(\nu,0,i)} - 1 \tag{33}$$

and

$$b_\nu(i) = \frac{\ln\tau_{480}(\nu,60^\circ,i)}{\ln\tau_{480}(\nu,0,i)} - 1\,. \tag{34}$$

It is clear from eqs. (33) and (34) that to construct eq. (32) one needs transmittance values for τ_{257} and τ_{480} at zenith angles of 0° and 60°, at each of the 40 pressure levels and for each of the first seven TOVS channels. These 1120 data values must be regenerated each time a new TOVS instrument package is launched.

Equation (32) now provides a general expression for the ozone transmittance curves, corresponding to total ozone amount Ω, for each of the first seven TOVS channels (which are the only ones affected by this absorption) at any zenith angle seen by the HIRS instrument and at any of the pressure levels.

4.2 Water-Vapor Continua

Water vapor exhibits absorption by two continua--the self-broadened, which depends on the square of the mixing-ratio, and the foreign-broadened, which depends on the first power of the mixing ratio (see, e.g., Roberts et al. 1976). As table 4 shows, the self-broadened continuum contributes in most of the infrared channels, but the foreign-broadened component is significant only for channels at wavelengths less than 8 µm. The references in table 6 are our sources for computations of continuum transmittances. As described in Weinreb and Hill (1980), we rearrange the equations in these references for computational convenience. Let $\tau_s(\nu,\theta,i)$ and $\tau_f(\nu,\theta,i)$ be the self- and foreign-broadened continuum transmittances for a path between the satellite and atmospheric level i with zenith angle θ. The equations we use are

$$\tau_s(\nu,\theta,i) = \exp\left[-a(\nu)\ \sec\theta \int_0^{P_i} pq^2\ \exp(b(\nu)/T)dp\right]$$

and

$$\tau_f(\nu,\theta,i) = \exp\left[-c(\nu)\ \sec\theta \int_0^{P_i} pq\ dp\right],$$

where the integrals are evaluated by the trapezoidal rule. The coefficients a, b, and c are channel-dependent and are derived from data in the references of table 6. No temperature dependence is formulated for the foreign-broadened continuum, in part because it is small and in part because it is not well understood.

Table 6.--References for continuum coefficients

Channel	Reference
1-8, 10	Roberts et al. (1976)
13-16	Burch et al. (1973)
17-19	Burch et al. (1971)

One will note that table 6 omits references for channels 11 and 12. These channels present a difficulty because they are located in a region of dense, strong spectral lines of water vapor. Burch et al. (1973) report that in this region their measured continuum coefficients contain a major contribution from lines centered within 5 cm^{-1} of the point of observation. Since this component of the absorption is already included in our line calculation (see section 3.3.1), it would be included twice if Burch's coefficients were used. Work is underway at NESS to derive more suitable continuum coefficients for these channels. In the meantime, absorption by the continua has been left out of the calculations in these channels. The resulting error is ameliorated somewhat by the following circumstances: Absorption by continua, particularly the self-broadened component, falls off more rapidly with altitude than does the absorption by spectral lines. This is a consequence of the continua's strong dependence on pressure and mixing ratio. Because the spectral lines absorb so strongly in these channels, most of the absorption in these vertical paths takes place at high altitudes. Therefore, the relative importance of the continuum is less than it would be if the absorption took place near the earth's surface.

4.3 Molecular Nitrogen

Molecular nitrogen has a collision-induced absorption band centered at 2330 cm^{-1}. The equation for calculating the transmittance due to this phenomenon is

$$\tau(\nu,\theta,i) = \exp\left[-d(\nu)\ \sec\theta\int_0^{P_i} p/T\ dp\right] .$$

As described in Weinreb and Hill (1980), this equation follows Burch et al. (1971), with the temperature dependence suggested by Susskind and Searl (1977). The coefficients $d(\nu)$ are channel-dependent and are derived from data in Shapiro and Gush (1966).

5. ALGORITHM FOR MICROWAVE CHANNELS

As with transmittances of spectral lines in the infrared, transmittances in the microwave region are computed from an efficient parameterization in lieu of time-consuming theoretical resonance-line calculations. As discussed in section 2.3.2, molecular oxygen dominates the absorption in the microwave channels, but absorption by water vapor must also be included in the calculations. For a channel with central frequency ν and for zenith angle θ, the oxygen transmittance $\tau_{O_2}(\nu,\theta,i)$ to atmospheric level i is given by the equation

$$\tau_{O_2}(\nu,\theta,i) = \exp\left[-\sec\ \theta\sum_{j=1}^{i} \alpha_{O_2}(\nu,j)\right] , \tag{35}$$

where

$$\alpha_{O_2}(\nu,j) = a_j(\nu) + b_j(\nu)\ T_j + c_j(\nu)T_j^2 , \tag{36}$$

and T is atmospheric temperature. The coefficients a, b, and c are determined off line from resonance-line calculations, as will be explained below. Note that the absorption coefficient $\alpha(\nu,j)$ accounts for absorption by the gas in the layer between levels j-1 and j. Note also that eq. (35) is of the form for monochromatic radiation. For water vapor the parameterization is similar to eqs. (35) and (36), but it involves mixing ratio as well as temperature:

$$\tau_{H_2O}(\nu,\theta,i) = \exp\left[-\sec\theta\sum_{j=1}^{i}\alpha_{H_2O}(\nu,j)\right] , \tag{37}$$

where

$$\alpha_{H_2O}(\nu,j) = d_j(\nu) + e_j(\nu)\,T_j + f_j(\nu)\,q_j + g_j(\nu)\,q_j\,T_j , \tag{38}$$

and where q_j is the water-vapor mixing ratio. The coefficients d, e, f, and g are determined off line. The overall atmospheric transmittance is then computed as the product of the two components; i.e.,

$$\tau(\nu,\theta,i) = \exp\sum_{j=1}^{i}\left\{-\left[\alpha_{O_2}(\nu,j) + \alpha_{H_2O}(\nu,j)\right]\sec\theta\right\} . \tag{39}$$

We determine the coefficients in these parameterizations off line by fitting eqs. (36) and (38) to results of resonance-line calculations on a sample of 32 atmospheric temperature and humidity profiles. (These profiles are not on the EDIS tape but are available on request from the authors.) The resonance-line calculations were developed for oxygen by Rosenkranz (1975) and for water vapor by Barrett and Chung (1962). For these calculations, each channel is subdivided into twenty 11-MHZ intervals. (Recall that each channel has a spectral bandpass of 220 MHz). Resonance-line calculations are done in each interval and then are averaged over the full bandpass. For each channel and level, multiple linear regression determines the three coefficients in eq. (36) from the resulting 32 pairs of α_{O_2} and T. For water-vapor, the four coefficients are determined from the 32 triplets of α_{H_2O}, T, and q.

Although the current operational procedures use eq. (39), a future improvement might be to recast the equation in a form not involving exponentials, which are time-consuming to calculate on the computer. To do this, we rewrite eq. (39) as

$$\tau(\nu,\theta,i) = \tau(\nu,\theta,i-1)\exp\left[-(\alpha_{O_2}(\nu,i) + \alpha_{H_2O}(\nu,i))\sec\theta\right].$$

In this equation the argument of the exponential is much smaller than unity for the thin layers considered here. Hence, the exponential can be approximated by the first two terms in a Maclaurin series; i.e.,

$$\tau(\nu,\theta,i) = \tau(\nu,\theta,i-1)\left[1-(\alpha_{O_2}(\nu,i) + \alpha_{H_2O}(\nu,i))\sec\theta\right].$$

The latter formula allows the transmittances to be calculated without exponentials.

6. EXAMPLES

This section presents examples of transmittances computed by the methods of this report. All are based on the subtropical atmosphere whose profiles of temperature and water-vapor mixing ratio appear in fig. 10. This atmosphere has 3.4 cm of precipitable water. The computations also require a value of the total ozone amount, for which we used 312 Dobson units. All calculations are done for a zenith angle of 0°. Figures 11-14 present profiles of calculated transmittances vs atmospheric pressure (altitude) for most channels of the HIRS, SSU and MSU. Not shown are transmittances for channels 18 and 19, which have less absorption than even channel 8; and for channel 9, which was not treated in this report.

What contribution does each atmospheric constituent make to the overall atmospheric transmittance? Figure 15 answers this question for channel 4 of the HIRS, displaying separate profiles of transmittance for each constituent, as well as the profile of overall atmospheric transmittance. Figures 16-19 isolate the transmittance profiles similarly for each constituent for, resp., channels 7, 10, and 15 of the HIRS and channel 4 of the MSU.

7. CONCLUSION

We have summarized the procedures used by the National Earth Satellite Service to produce atmospheric transmittance functions for the TIROS Operational Vertical Sounder. They are composite transmittances in that they include all atmospheric gases that contribute to the absorption in each channel. While these transmittance calculations are more comprehensive than those for earlier sounders, they still satisfy the dual requirements of operational data processing: accuracy and efficiency. An IBM-compatible magnetic tape of the software necessary to implement these procedures can be obtained from NOAA's Environmental Data and Information Service at the address given in the Introduction of this report.

ACKNOWLEDGEMENTS

We acknowledge the work of M.W. Chalfant and M.L. Hill of NOAA/NESS and Dr. C.A. Dean of Systems and Applied Science Corp. (presently with S.M. Systems and Research, Inc.), for converting the methods described in this report to operational FORTRAN code. M.L. Hill is also to be credited for preparing figs. 11-19 of this report. Dr. N.C. Grody and H.M. Woolf assisted in developing the algorithm for the MSU channels. We are grateful to Dr. D.R. Pick of the British Meteorological Office for supplying transmittances calculated line by line for the SSU. We are indebted to Dr. E.R. Westwater of NOAA/ERL and Dr. C.M. Hayden of NOAA/NESS for their thorough and helpful reviews of this report. We appreciate the patience of Ms. Kay Collins, who typed, and retyped, the manuscript.

REFERENCES

Arking, A. (Goddard Space Flight Center, National Aeronautics and Space Administration, Greenbelt, MD), 1977, (personal communication).

Banks, P.M. and G. Kockarts, 1973: Aeronomy, Part A. Academic Press, New York, N.Y., 430 pp.

Barrett, A.H. and V.K. Chung, 1962: A method for the determination of high-altitude water-vapor abundance from ground-based microwave observations. J. Geophys. Res. 67, 4259-4266.

Burch, D.E., D.A. Gryvnak, R.R. Patty and C.E. Bartky, 1969: Absorption of infrared radiant energy by CO_2 and H_2O. IV. Shapes of collisioned-broadened CO_2 lines. J. Opt. Soc. Am., 59, 267-280.

Burch, D.E., D.A. Gryvnak, and J.D. Pembrook, 1971: Investigation of the absorption of infrared radiation by atmospheric gases: water, nitrogen, nitrous oxide. Semi-Annual Technical Report. No. 2, AFCRL-71-0124, Philco-Ford Corporation, Aeronutronic Division, Newport Beach, CA, 25 pp.

Burch, D.E., D.A. Gryvnak, and G.H. Piper, 1973: Infrared absorption by H_2O and N_2O. Final Contract Report, AFCRL-TR-73-0530, Philco-Ford Corporation, Aeronutronic Division, Newport Beach, CA. 92663, 26 pp.

Burch, D.E., E.B. Singleton, W.L. France, and D. Williams, 1960: Infrared absorption by minor atmospheric constituents. Final Report, AFCRL Contract No. AF 19(604)-2633, The Ohio State University Research Foundation, Columbus, Ohio, 65 pp.

Carter, C.J., R.L. Mitchell, and E.E. Reber, 1968: Oxygen absorption measurements in the lower atmosphere. J. Geophys. Res., 73, 3113-3120.

Cicerone, R.J., J.D. Shetter, D.H. Stedman, T.J. Kelly, and S.C. Liu, 1978: Atmospheric N_2O: measurements to determine its sources, sinks, and variations. J. Geophys. Res., 83, 3042-3050.

COESA (U.S. Committee on Extension to the Standard Atmosphere) 1962: U.S. Standard Atmosphere, 1962. U.S. Government Printing Office, Washington, D.C., 278 pp.

Drayson, S.R., 1966: Atmospheric transmission in the CO_2 bands between 12 μ and 18 μ. Appl. Opt., 5, 385-391.

Fleming, H.E., 1981: A new numerical treatment of the source function in the radiative transfer equation. Preprint Volume, Fourth Conf. on Atmospheric Radiation, June 16-18, 1981, Toronto, Canada. Amer. Meteorol. Soc., Boston, MA. pp. 9-12.

Fleming, H.E. and L.M. McMillin, 1977: Atmospheric transmittance of an absorbing gas. 2: a computationally fast and accurate transmittance model for slant paths at different zenith angles. Appl. Opt. 16, 1366-1370.

Fleming, H.E. and W.L. Smith, 1972: Inversion techniques for remote sensing of atmospheric temperature profiles. In Temperature: Its Measurement and Control in Science and Industry, H.H. Plumb, ed., (Instrument Society of America, Pittsburgh, 1972), Vol. 4, Part 3, pp. 2239-2250.

Goody, R.M., 1964: Atmospheric Radiation, I: Theoretical Basis. Clarendon Press, Oxford, U.K., 436 pp.

Grody, N.C., 1976: Remote sensing of atmospheric water content from satellites using microwave radiometry. IEEE Trans. Antennas and Propagation, 24, 155-162.

Kneizys, F.X., E.P. Shettle, E.P. Gallery, J.H. Chetwynd, Jr., L.W. Abreu, J.E.A. Selby, R.W. Fenn, and R.A. McClatchey, 1980: Atmospheric transmittance/radiance: computer code LOWTRAN 5. Air Force Geophysics Laboratory Report AFGL-TR-80-0067, Air Force Geophysics Laboratory, Hanscom AFB, Massachusetts 01731, 233 pp.

Kunde, V.G. and W.C. Maguire, 1974: Direct integration transmittance model. J. Quant. Spectrosc. Radiat. Transfer, 14, 803-817.

Kyle, T.G. and A. Goldman, 1975: Atlas of computed infrared atmosopheric absorption spectra. NCAR Tech. Note STR-112, National Center for Atmospheric Research, Boulder, CO, 72 pp.

London, J. 1962: The distribution of total ozone over the Northern Hemisphere. Sun at Work, 7, 11-12.

London, J. 1978: Distribution of atmospheric ozone and how it is measured. Special Technical Publication 653, Am. Soc. for Testing and Materials, Philadelphia, PA, 339-364.

Matthias, A.D., A.M. Blackmer, J.M. Bremner, 1979: Diurnal variability in the concentration of nitrous oxide in surface air. Geophys. Res. Lett., 6, 441-443.

McClatchey, R.A., W.S. Benedict, S.A. Clough, D.E. Burch, R.F. Calfee, K. Fox, L.S. Rothman, and J.S. Garing, 1973: AFCRL atmospheric absorption line parameters compilation. AFCRL-TR-73-0096, Air Force Cambridge Research Laboratories, L.G. Hanscom Field, Bedford, MA, 78 pp.

McMillin, L.M. and H.E. Fleming, 1976: Atmospheric transmittance of an absorbing gas: a computationally fast and accurate transmittance model for absorbing gases with constant mixing ratios in inhomogeneous atmospheres. Appl. Opt. 15, 358-363.

McMillin, L.M., H.E. Fleming, A. Arking, and D. Chesters 1980: Accuracies of three computationally efficient algorithms for computing atmospheric transmittances. Appl. Opt. 19, 2267-2268.

McMillin, L.M., H.E. Fleming, and M.L. Hill, 1979: Atmospheric transmittance of an absorbing gas. 3: A computationally fast and accurate transmittance model for absorbing gases with variable mixing ratios. Appl. Opt., 18, 1600-1606.

McMillin, L.M., D.Q. Wark, J.M. Siomkajlo, P.G. Abel, A. Werbowetski, L.A. Lauritson, J.A. Pritchard, D.S. Crosby, H.M. Woolf, R.C. Luebbe, M.P. Weinreb, H.E. Fleming, F.E. Bittner, and C.M. Hayden, 1973: Satellite infrared soundings from NOAA spacecraft. NOAA Technical Report NESS 65, National Oceanic and Atmospheric Administration, U.S. Department of Commerce, Washington, D.C. 112 pp.

Migeotte, M., L. Neven, J. Swensson, 1957: The solar spectrum from 2.8 to 23.7 microns. Final Report - Phase A (Part II), Air Force Cambridge Research Center Contract No. AF 61(514)-432, Institute D'Astrophysique de L'Universite de Liege and Observatoire Royal de Belgique, Belgium.

Miller, D.E., J.L. Brownscombe, G.P. Carruthers, D.R. Pick, and K.H. Stewart, 1980: Operational temperature sounding of the stratosphere. Phil. Trans. R. Soc. Lond. A296, 65-71.

Murcray, D.G., F.H. Murcray, W.J. Williams, J.N. Brooks, D.Q. Wark, and F.L. VanCleef, 1971: Atmospheric transmittances in the 15 μm carbon dioxide band and their application to remote temperature sounding. 52nd Annual Meeting of Amer. Geophys. Union, Washington, D.C.

Neuendorffer, A.C., 1977: Rapid atmospheric transmittance through fast Fourier convolution. J. Opt. Soc. Am., 67, 1376.

Pick, D.R. (Meteorological Office, London Road, Bracknell, Berkshire, U.K.), 1980 (personal communication).

Planet, W.G. (National Environmental Satellite Service, National Oceanic and Atmospheric Administration, U.S. Department of Commerce, Washington, D.C.) 1975 (personal communication).

Roberts, R. E., J.E.A. Selby, and L.M. Biberman, 1976: Infrared continuum absorption by atmospheric water vapor in the 8-12 μm window. Appl. Opt., 15, 2085-2090.

Rosenkranz, P.W., 1975: Shape of the 5 mm oxygen band in the atmosphere. IEEE Trans. on Antennas and Propagation, Vol. AP-23, 498-506.

Rothman, L.S. and R.A. McClatchey, 1976: Updating of the AFCRL atmospheric absorption line parameters compilation. Appl. Opt., 15, 2616.

Schwalb, A., 1978: The TIROS-N/NOAA A-G satellite series. NOAA Tech. Memo NESS 97, National Oceanic and Atmospheric Administration, Washington, D.C., 75 pp.

Shapiro, M.M. and H.P. Gush, 1966: The collision-induced fundamental and first overtone bands of oxygen and nitrogen. Can. J. Phys., 44, 949-963.

Smith, W.L. 1969: A polynomial representation of carbon dioxide and water vapor transmission. ESSA Technical Report NESC 47, Environmental Science Services Administration, U.S. Department of Commerce, Washington, D.C., 20 pp.

Smith, W.L. and P.G. Abel (National Environmental Satellite Service, National Oceanic and Atmospheric Administration, U.S. Department of Commerce, Washington, D.C), 1974 (personal communication).

Smith, W.L. and H.M. Woolf, 1976: The use of eigenvectors of statistical covariance matrices for interpreting satellite sounding radiometer observations. J. Atmos. Sci., 33, 1127-1140.

Smith, W.L., H.M. Woolf, C.M. Hayden, D.Q. Wark, and L.M. McMillin, 1979: The TIROS-N operational vertical sounder. Bull. Am. Meteor. Soc., 60, 1177-1187.

Stowe, L.L., 1974: Effects of particulate matter on the radiance of terrestrial infrared radiation; results. J. Atmos. Sci., 31, 755-767.

Stowe, L.L. and H.E. Fleming, 1980: The error in satellite retrieved temperature profiles due to the effects of atmospheric aerosol particles. Remote Sensing of Environment, 9, 57-64.

Susskind, J. and J.E. Searl, 1977: Atmospheric absorption near 2400 cm^{-1}. J. Quant. Spectrosc. Radiat. Transfer, 18, 581-587.

Susskind, J. and J.E. Searl, 1978: Synthetic atmospheric transmittance spectra near 15 and 4.3 μm. J. Quant. Spectrosc. Radiat. Transfer, 19, 195-215.

Weinreb, M.P., 1977: Sensitivity of satellite retrievals of temperature to errors in estimates of tropospheric water vapor. Journal of Applied Meteorology, 16, 605-613.

Weinreb, M.P. and M.L. Hill, 1980: Calculation of atmospheric radiances and brightness temperatures in infrared window channels of satellite radiometers. NOAA Tech. Rept. NESS 80, National Oceanic and Atmospheric Administration, U.S. Department of Commerce, Washington, D.C., 40 pp.

Weinreb, M.P. and A.C. Neuendorffer, 1973: Method to apply homogeneous-path transmittance models to inhomogeneous atmospheres. J. Atmos. Sci., 30, 662-666.

Weinreb, M.P., W.G. Planet, and G.D. Jones, 1977: Transmittance of the atmosphere to infrared solar radiation. J. Opt. Soc. Am., 67, 1377.

Winters, B.H., S. Silverman, and W.S. Benedict, 1964: Line shape in the wing beyond the band head of the 4.3 μ band of CO_2. J. Quant. Spectros. Radiat. Transfer, 4, 527-537.

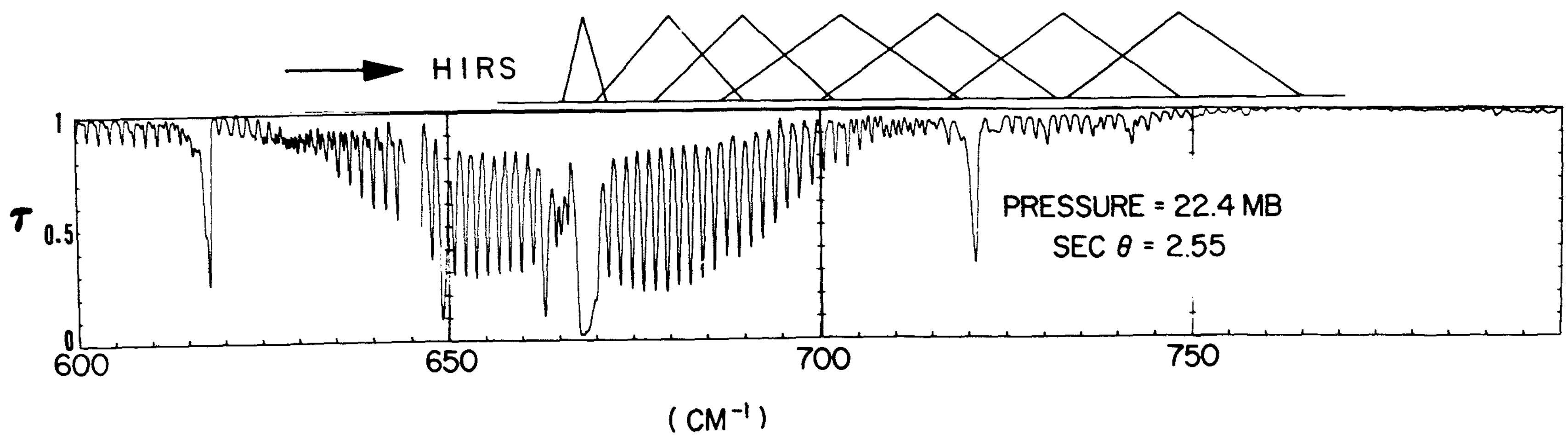

Figure 1.--Locations of idealized spectral intervals of HIRS channels 1-7 with atmospheric spectrum (Murcray et al. 1971) measured from balloon at altitude of 22.4 mb. Ordinate is in units of transmittance.

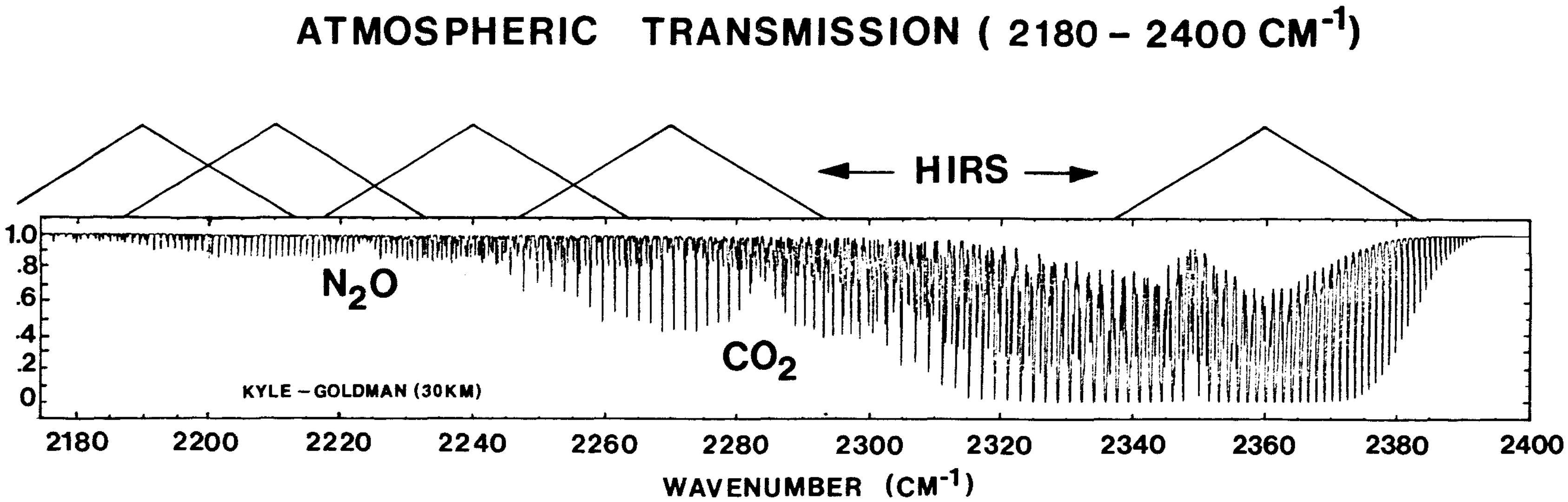

Figure 2.-- As in fig. 1 for HIRS channels 13-17. Spectrum calculated by Kyle and Goldman (1975) for a vertical path from altitude of 30 km to space.

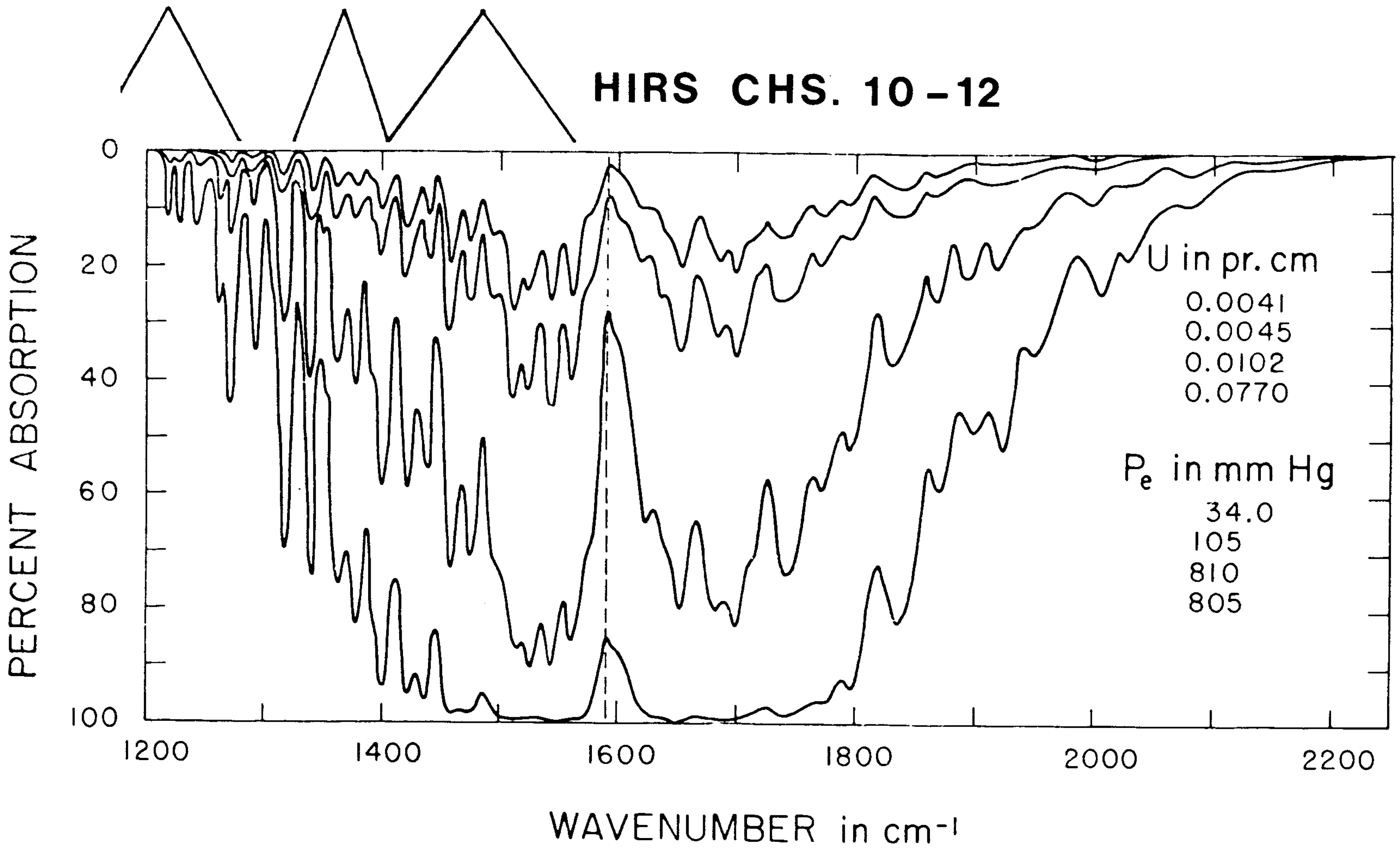

Figure 3.-- Locations of idealized spectral intervals of HIRS channels 10-12 with low-resolution laboratory spectra (Burch et al. 1960). U refers to water-vapor amount. P_e is pressure of broadening gas (nitrogen). The four curves correspond to the four sets of values of U and P_e listed on the figure.

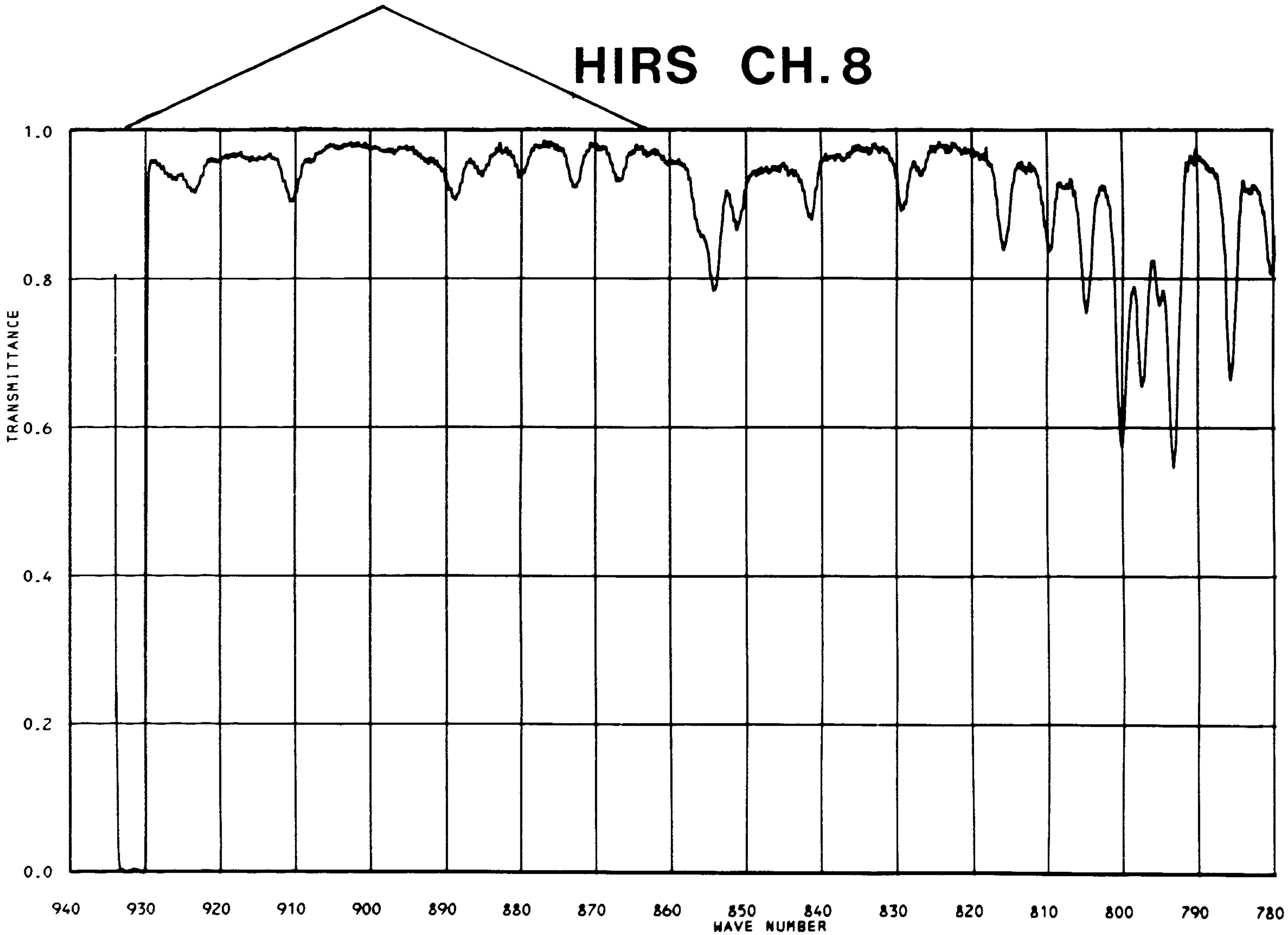

Figure 4.--As in fig. 1, for HIRS channel 8. Atmospheric spectrum from Weinreb and Hill (1980). (The "feature" between 930 and 935 cm^{-1} is calibration, not atmospheric absorption.)

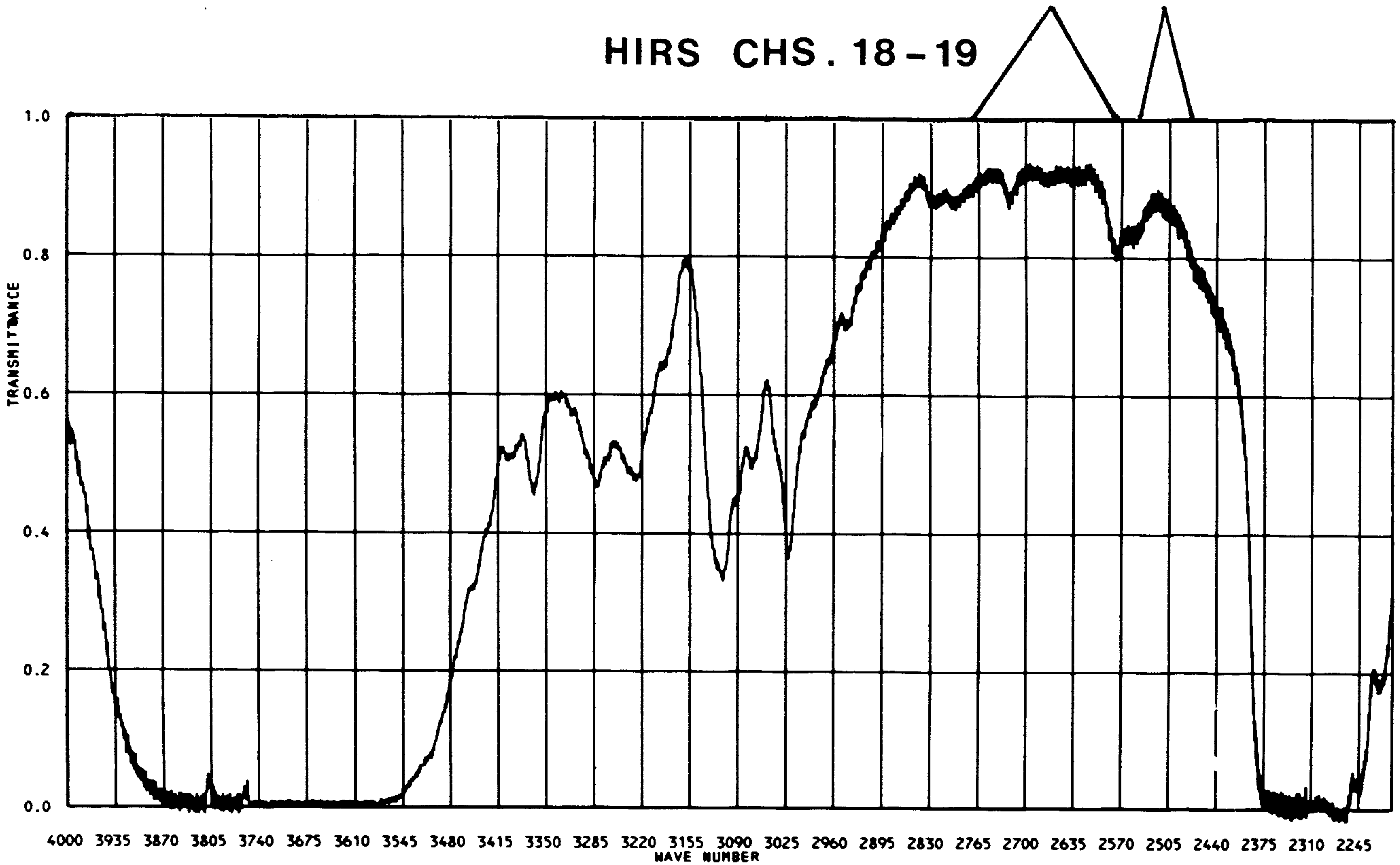

Figure 5.--As in fig. 1, for HIRS channels 18-19. Atmospheric spectrum taken by W.G. Planet (1975) with solar radiation from McMath Solar Telescope at Kitt Peak National Observatory. Solar zenith angle was 13.6°.

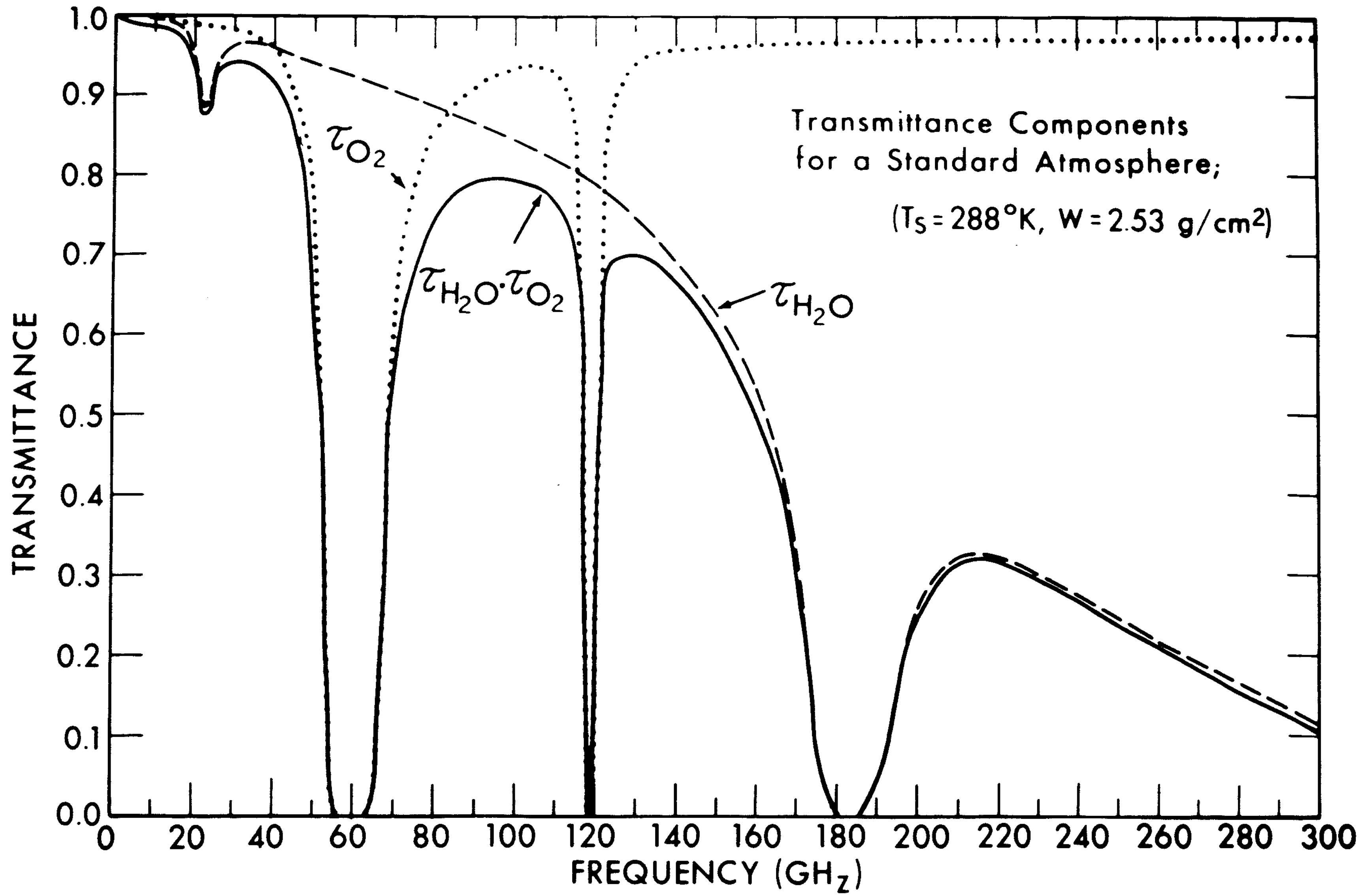

Figure 6.--Transmittances in microwave region calculated for path between surface and space for O_2, H_2O, and for their product (from Grody (1976)).

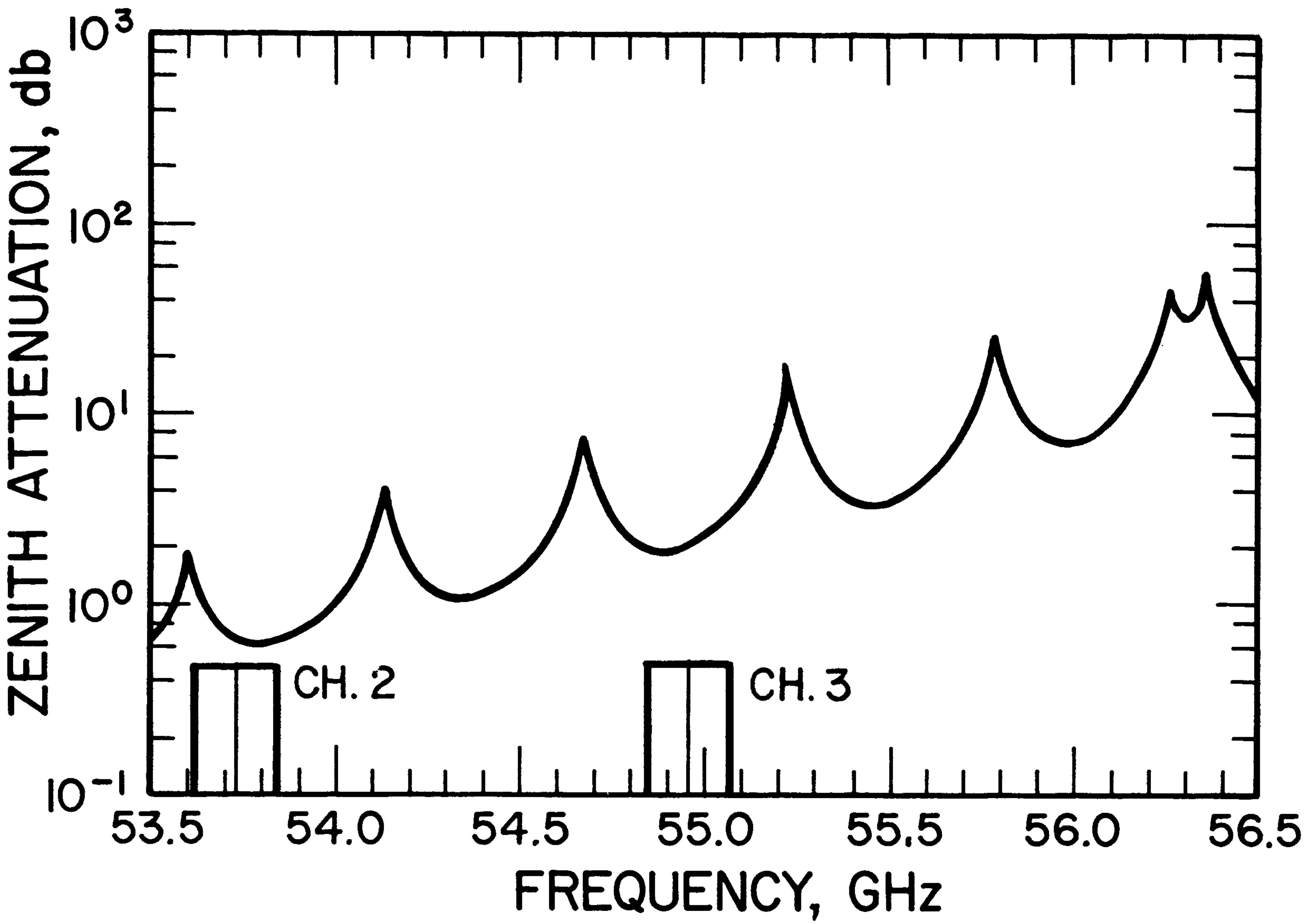

Figure 7.--Locations of spectral intervals of MSU channels 2-3 with atmospheric spectrum adapted from fig. 3 of Carter et al. (1968). Ordinate is in units of attenuation (db).

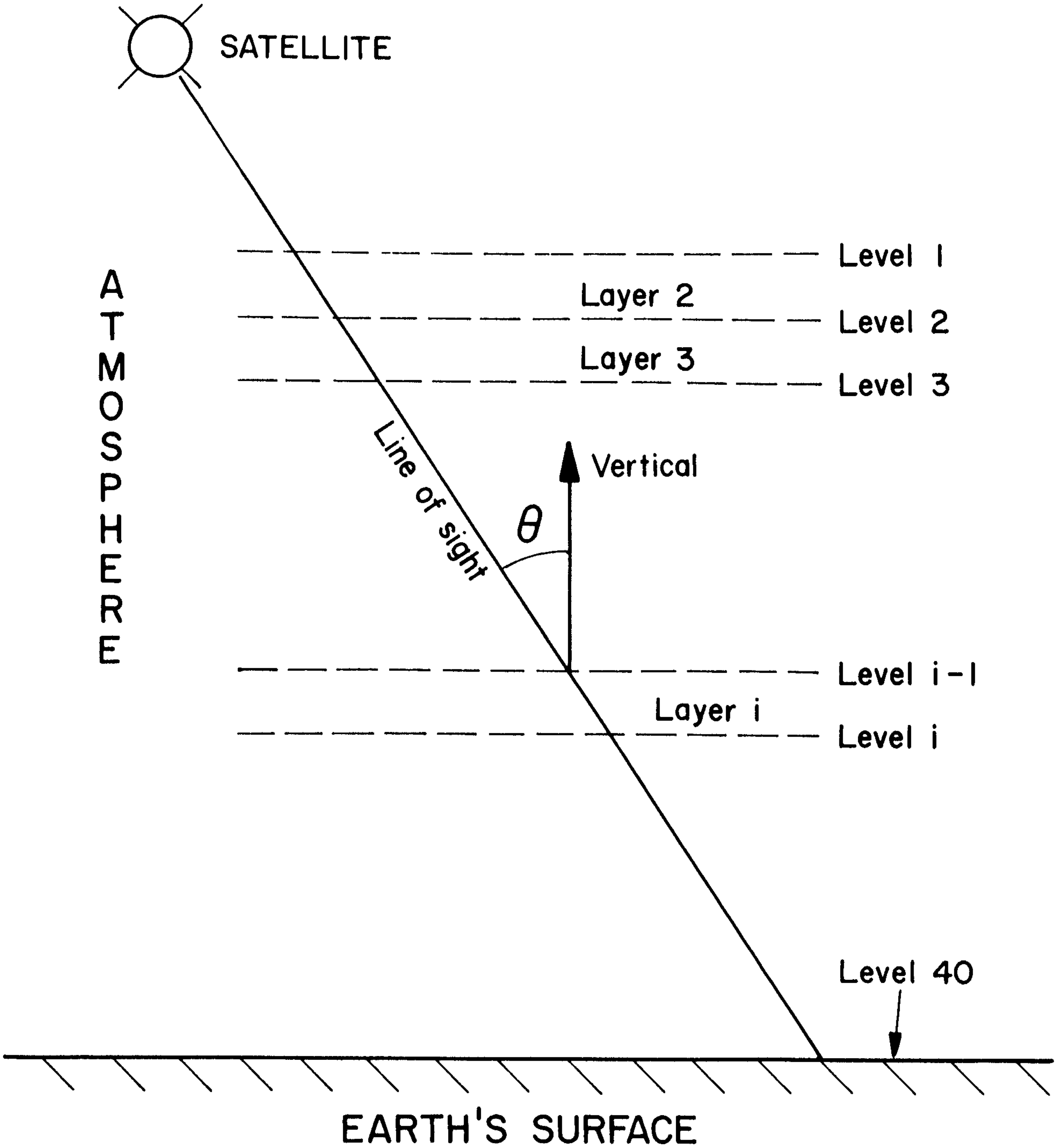

Figure 8.--Coordinate system in the atmosphere.

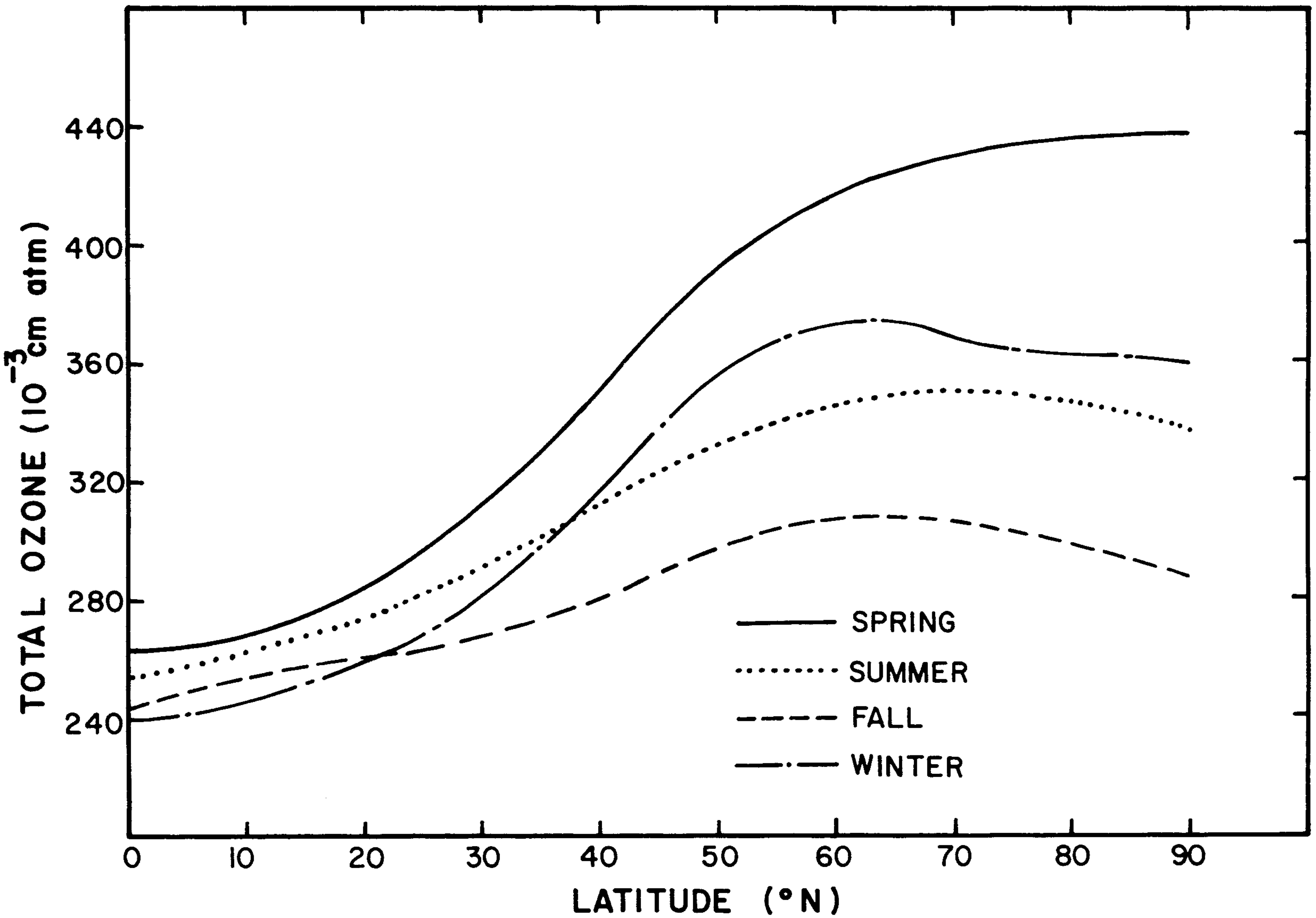

Figure 9.--Total ozone vs latitude (from London (1962)). Given season and latitude, one can obtain a value of total ozone.

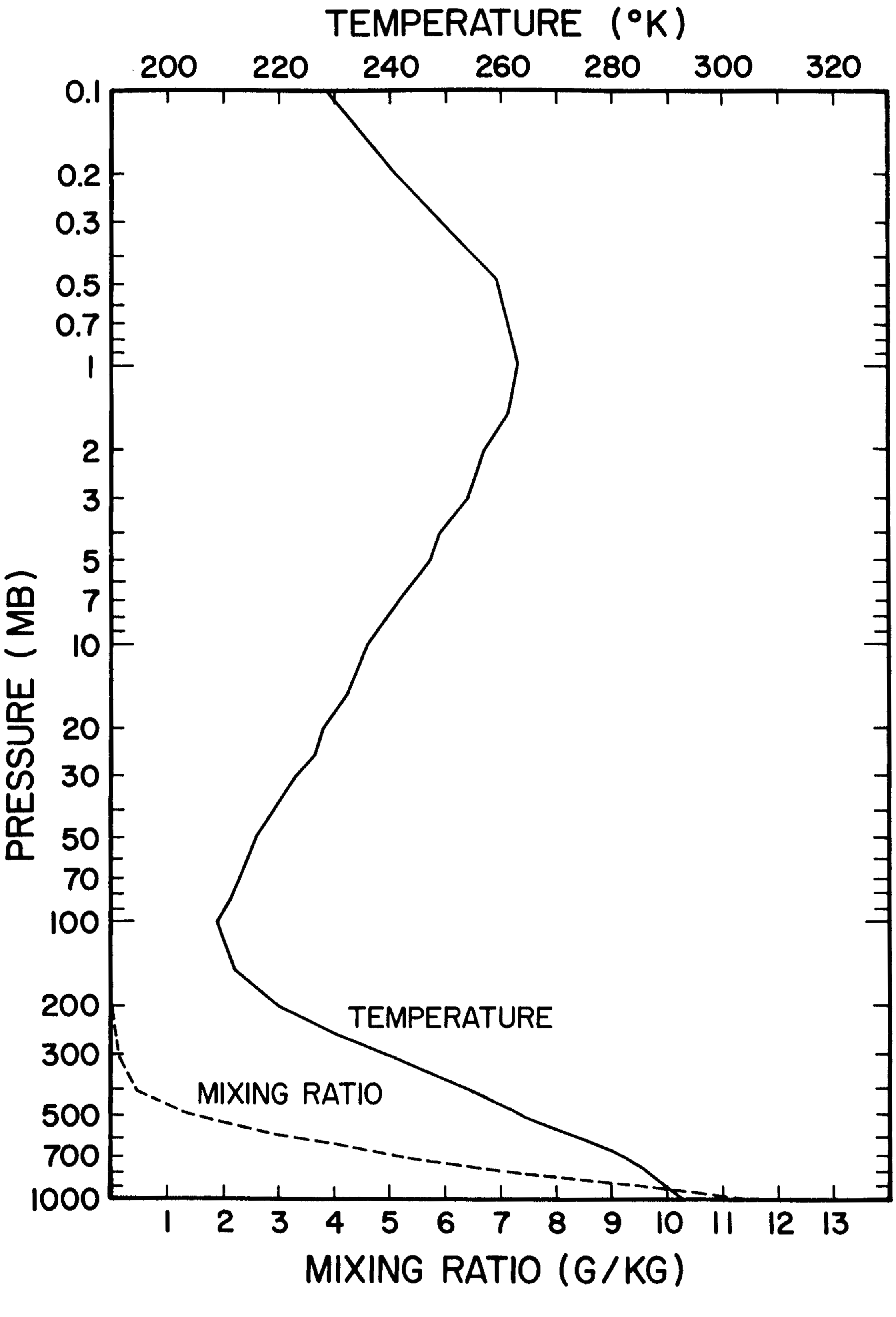

Figure 10.--Profiles of temperature and water-vapor mixing ratio.

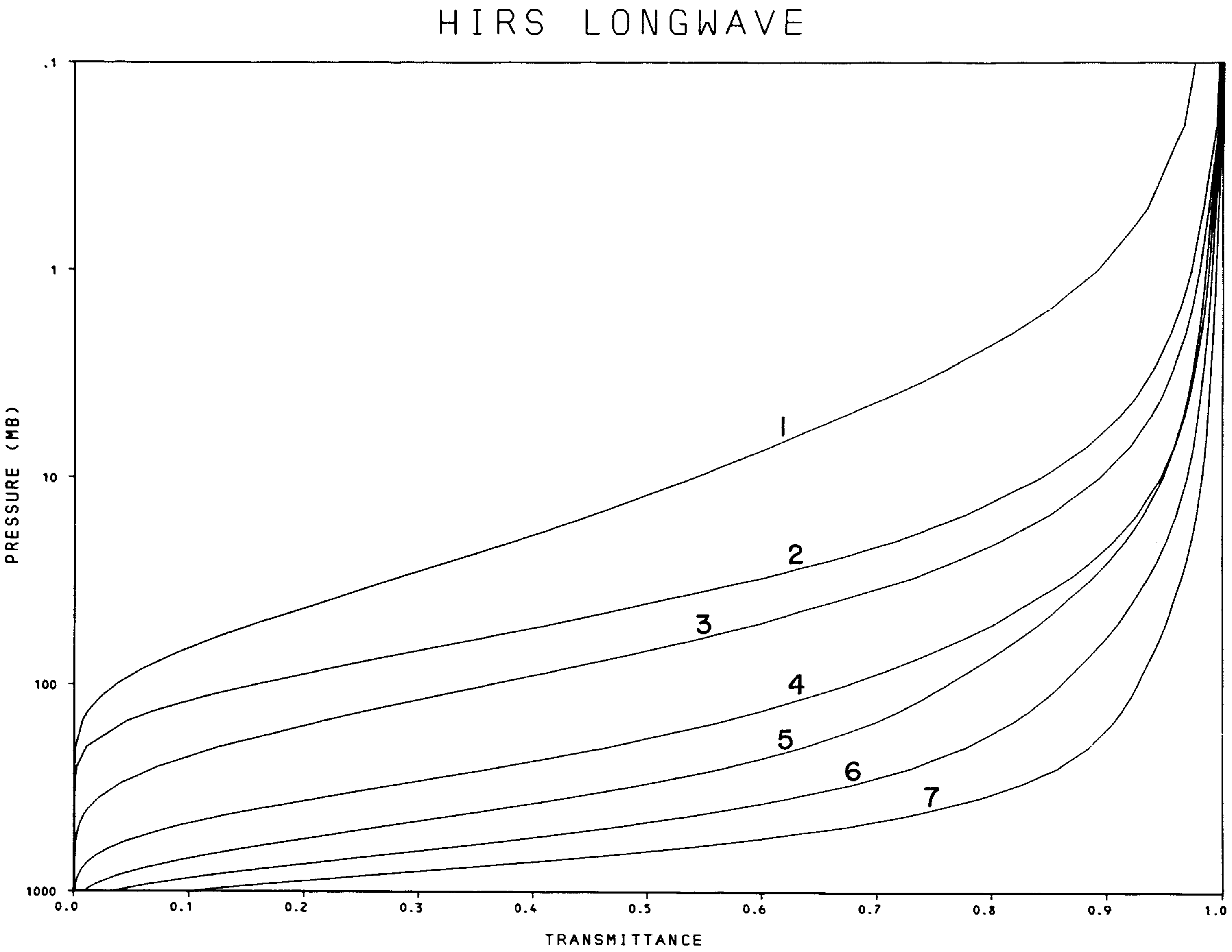

Figure 11.--Profiles of transmittance vs atmospheric pressure for HIRS channels 1-7.

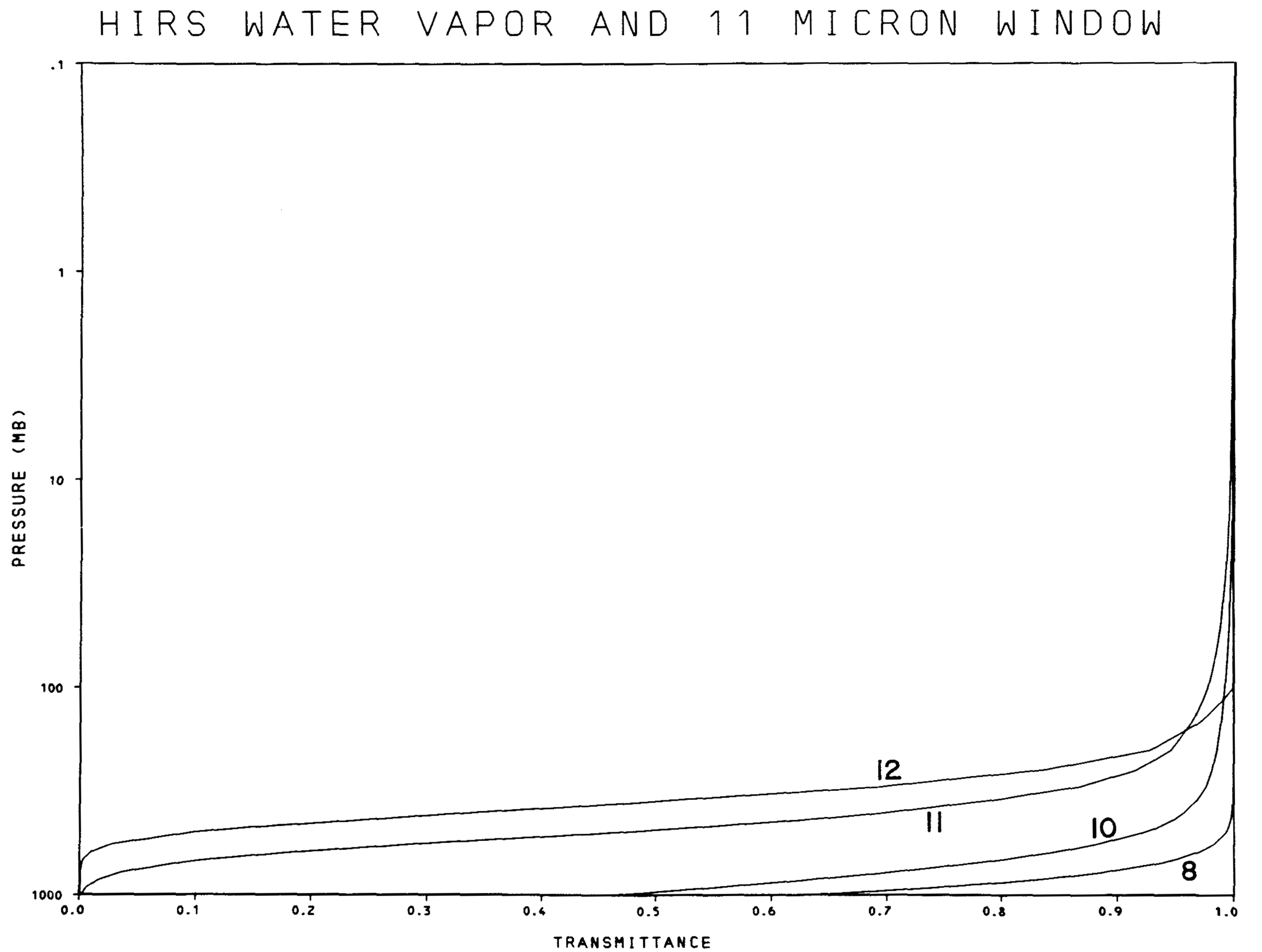

Figure 12.--As in fig. 11, for HIRS channels 8, 10-12.

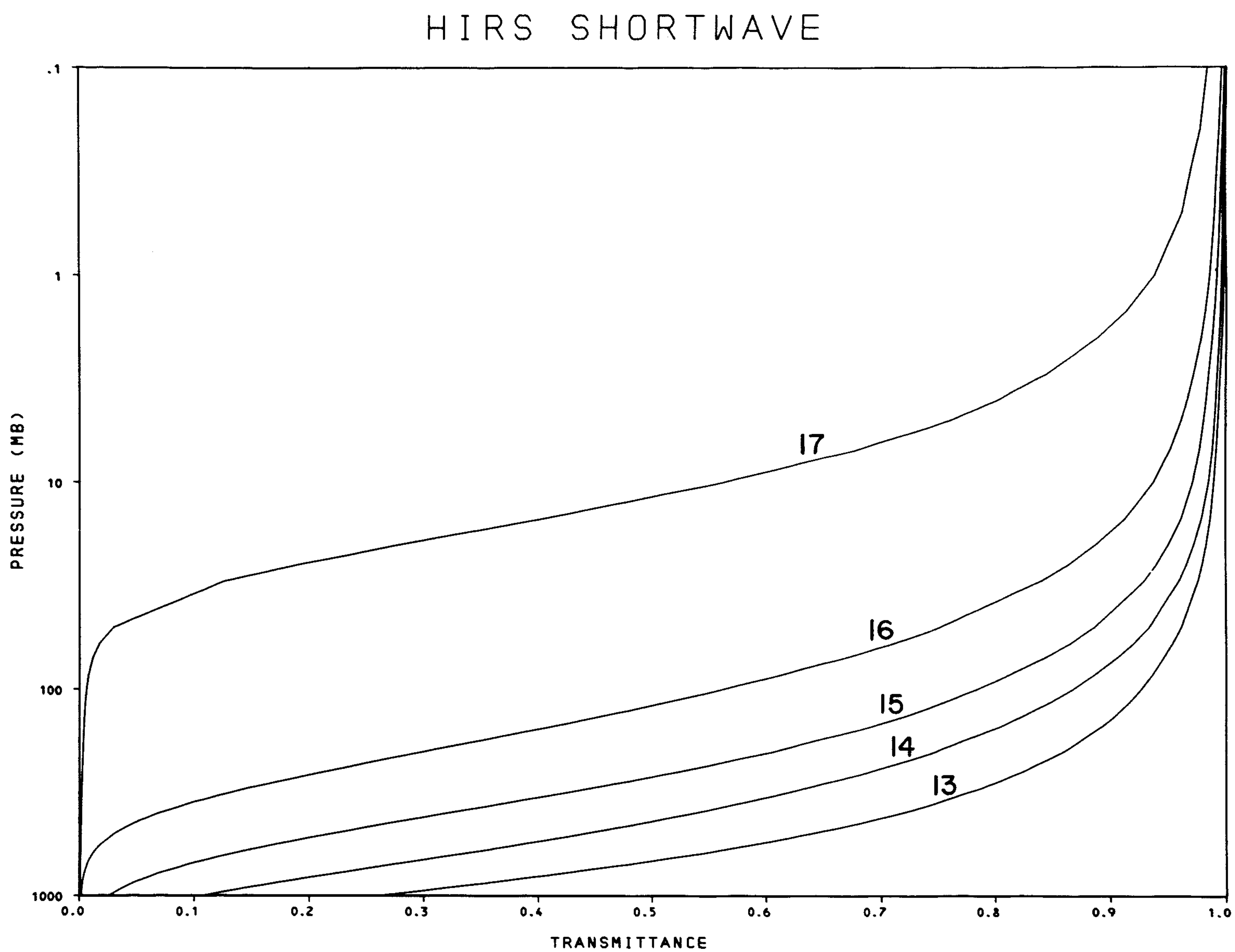

Figure 13.--As in fig. 11, for HIRS channels 13-17.

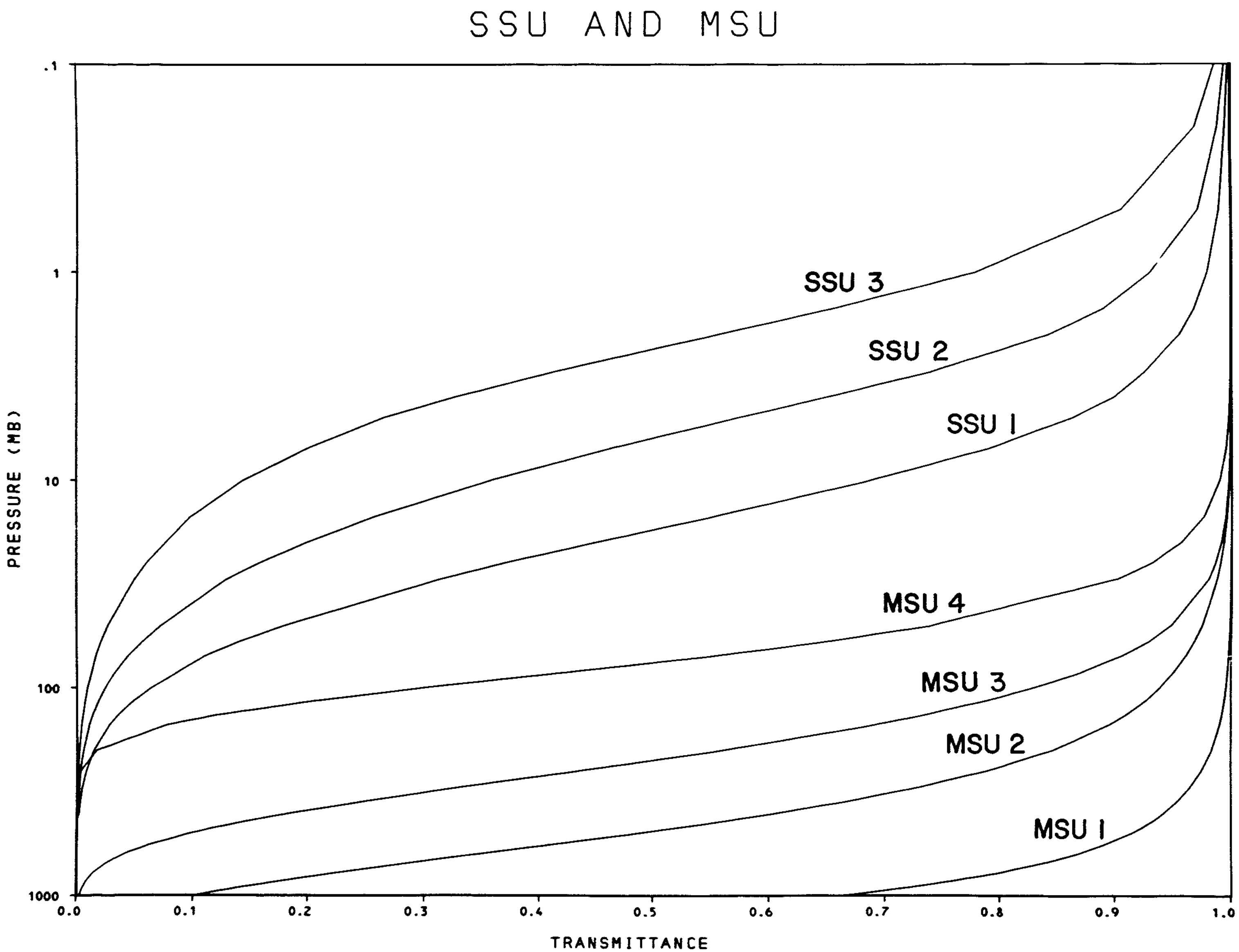

Figure 14.--As in fig. 11, for the SSU and MSU channels.

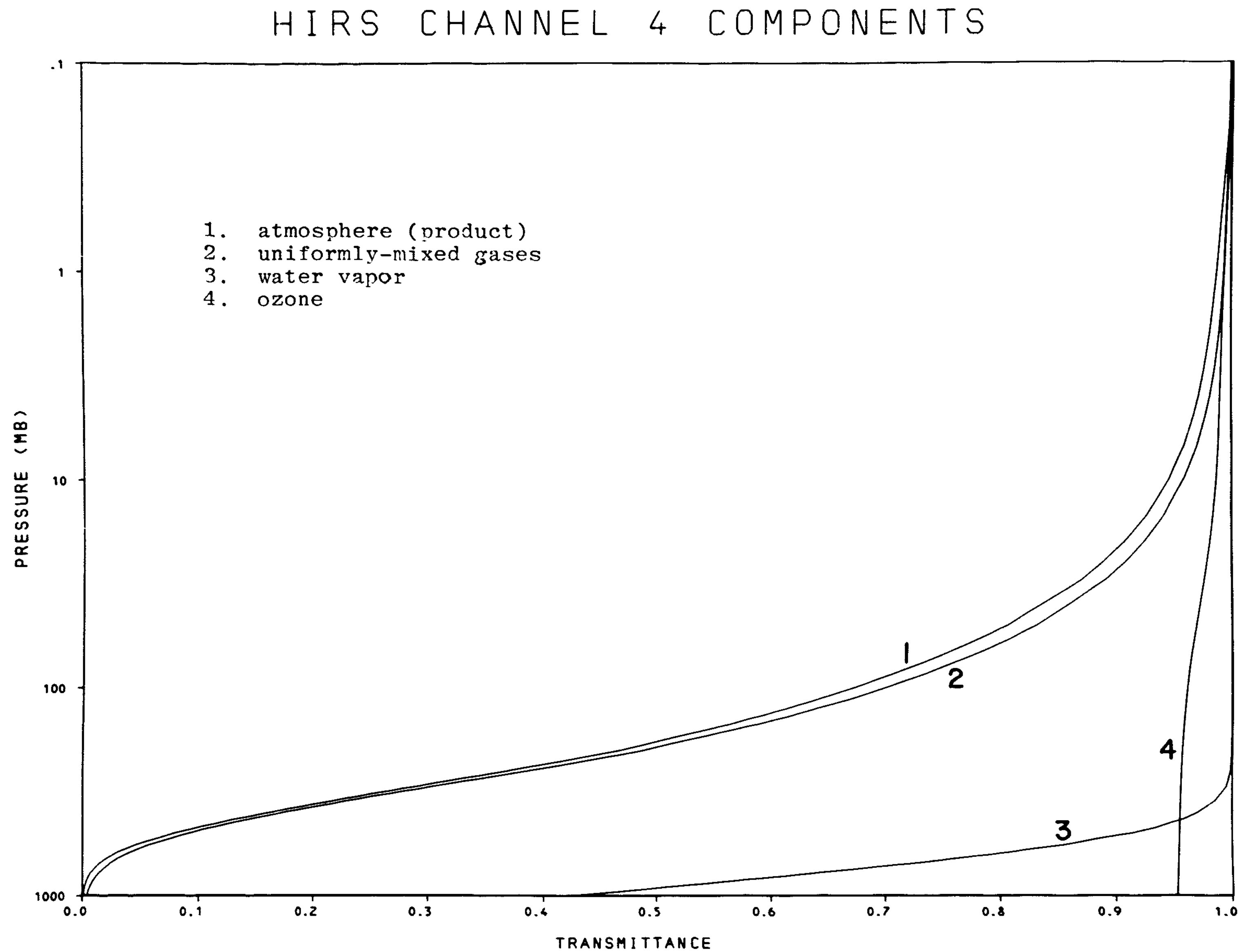

Figure 15.--Profiles of transmittances vs atmospheric pressure for each constituent. Atmospheric transmittance is product of transmittances of all constituents. Computations are for HIRS channel 4.

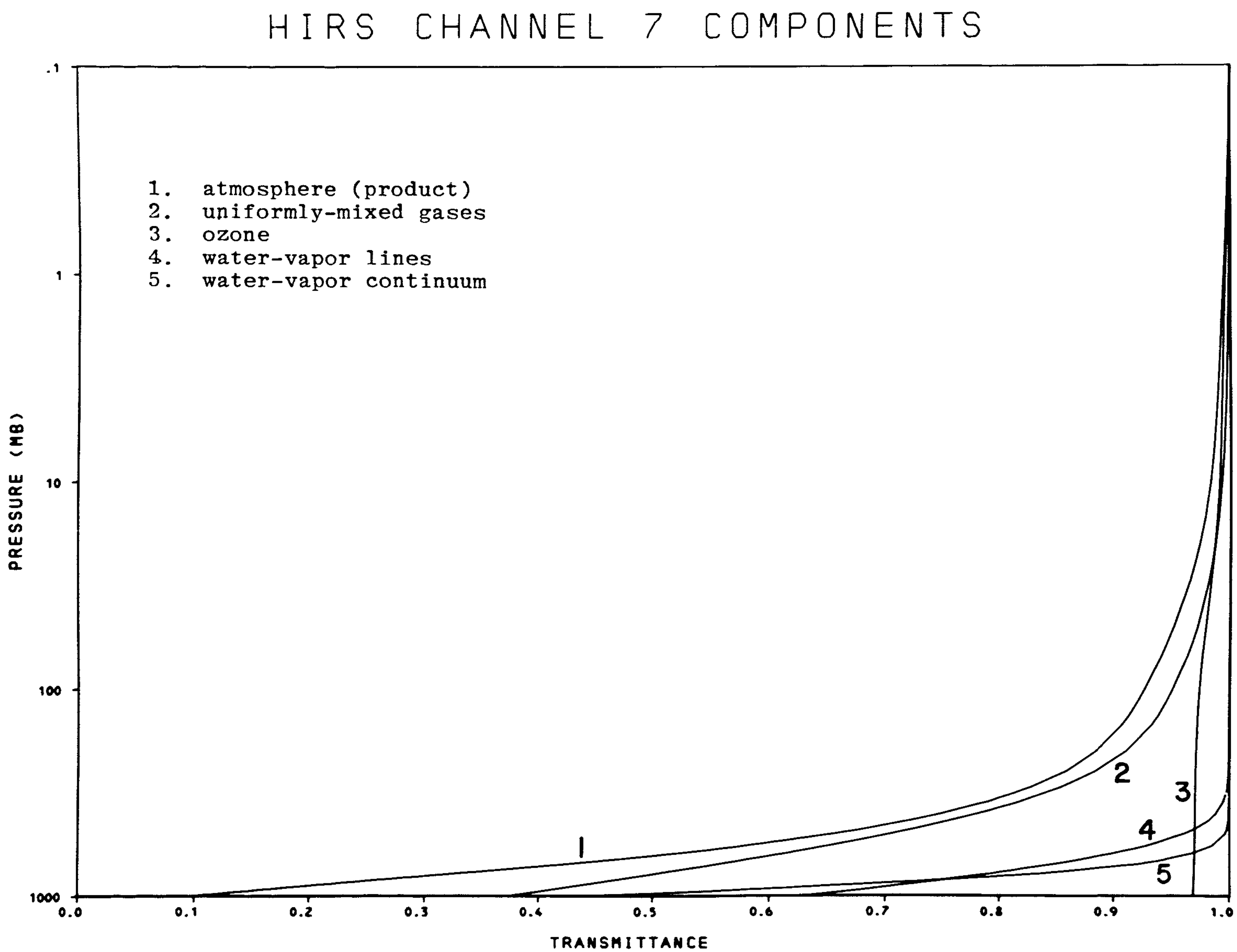

Figure 16.--As in fig. 15, for HIRS channel 7.

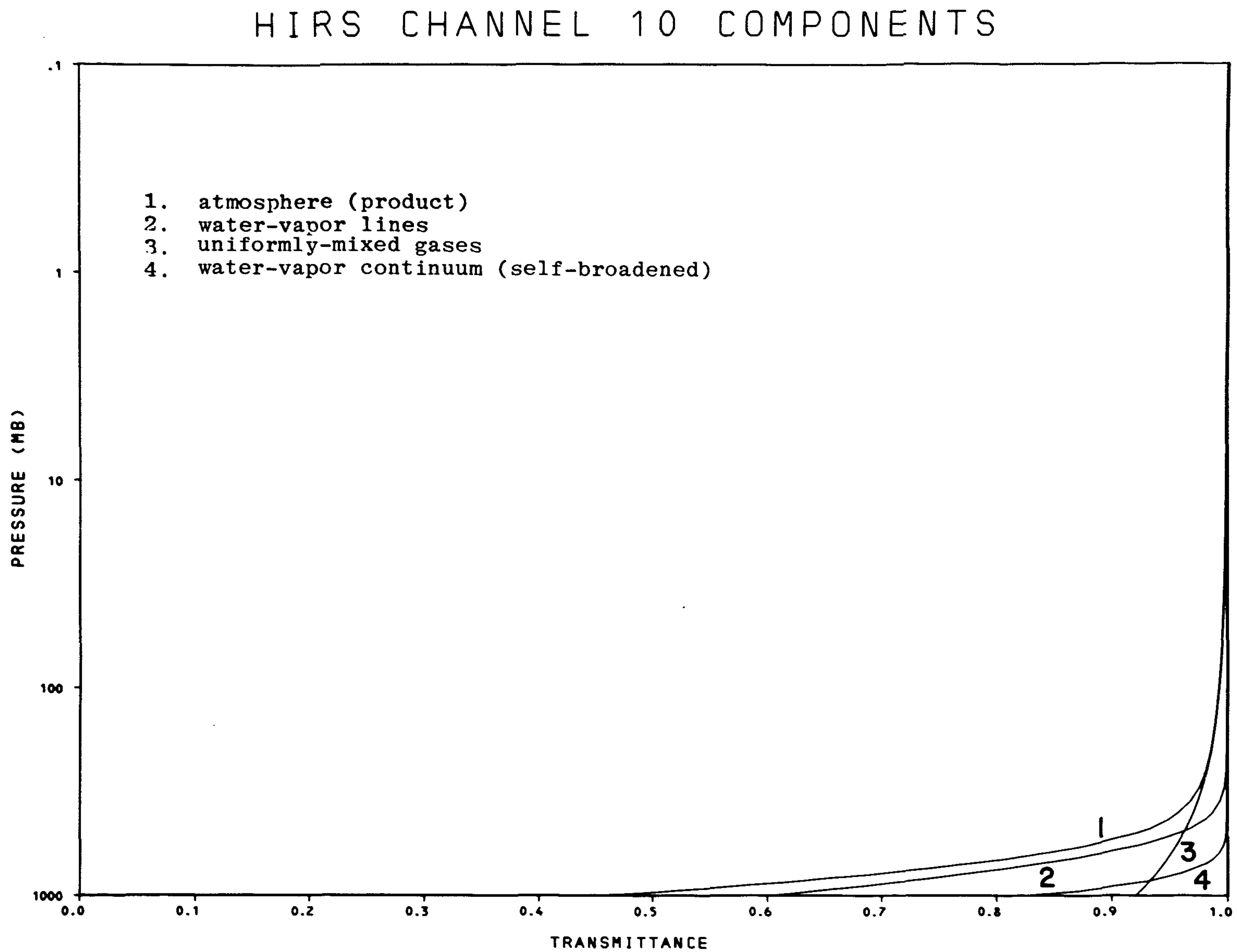

Figure 17.--As in fig. 15, for HIRS channel 10.

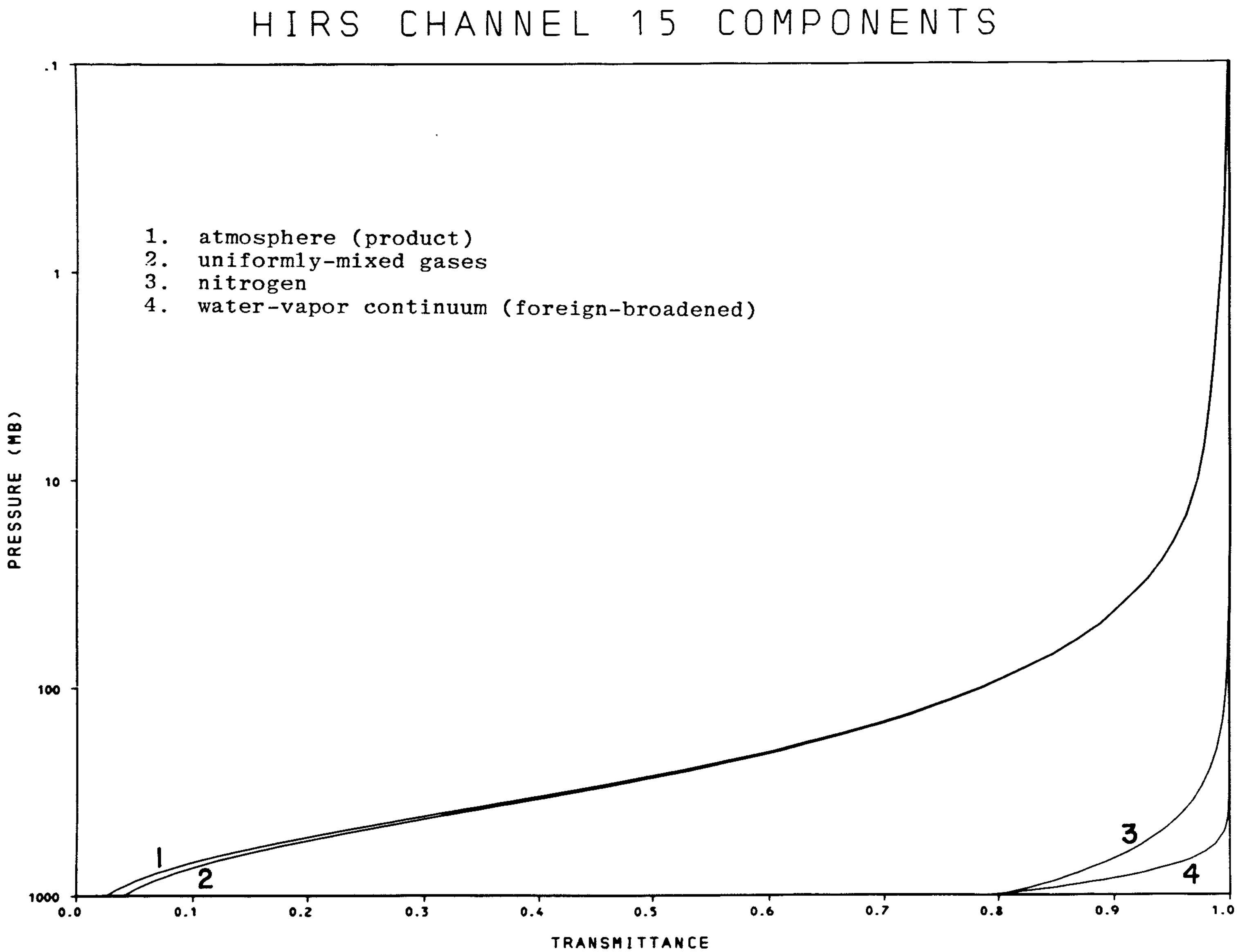

Figure 18.--As in fig. 15, for HIRS channel 15.

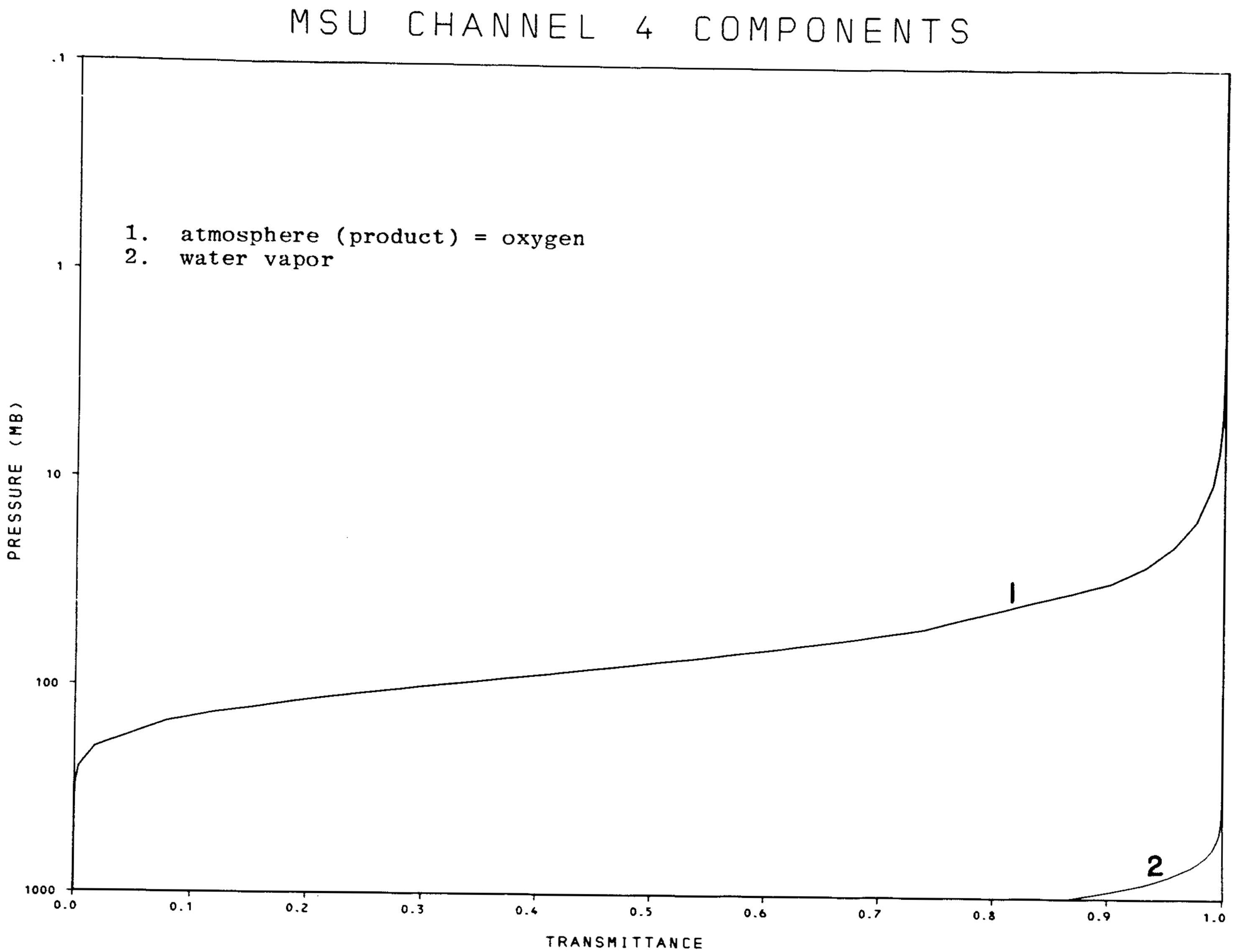

Figure 19.--As in fig. 15, for MSU channel 4.

APPENDIX A. THE 19 TEMPERATURE PROFILES

Table A1 lists the temperature profiles that are the basis for the computations of coefficients for the rapid transmittance algorithm (eqs. (22) and (25)) for the uniformily-mixed gases. Note that the first profile is the U.S. Standard Atmosphere (COESA 1962). Profiles 2-7 are displacements of the Standard Atmosphere by ± 10, ± 20, and ± 30°K at all levels. Only the first sixteen of these profiles are actually used in producing the coefficients. The last three profiles are used in checking the validity of the coefficients.

Table A1.--Temperature profiles.
Note that profiles 2-7 are displacements of the Standard Atmosphere by $\pm$ 10, $\pm$ 20, and $\pm$ 30°K.

PRESSURE (mb)	STAND. ATMOS.	8	9	10	11	12	13	14	15	16
.01	180.7	207.0	206.0	188.0	210.0	217.0	209.0	192.0	179.0	207.0
.04	211.6	229.0	228.0	214.0	231.0	237.0	229.0	216.0	211.0	229.0
.07	226.0	238.0	237.0	224.0	239.0	245.0	237.0	226.0	224.0	238.0
.1	235.5	244.0	243.0	231.0	244.0	250.0	242.0	232.0	232.0	244.0
.4	264.6	263.0	262.0	256.0	264.0	271.0	262.0	257.0	264.0	262.0
.7	270.6	260.0	259.0	266.0	267.0	274.0	271.0	267.0	277.0	259.0
1.0	270.6	254.0	252.0	266.0	267.0	274.0	273.0	267.0	267.0	252.0
1.3	267.2	246.0	243.0	262.0	260.0	270.0	268.0	262.0	263.0	244.0
1.6	262.6	240.0	236.0	258.0	256.0	266.0	265.0	258.0	260.0	237.0
2	257.9	233.0	230.0	254.0	250.0	263.0	262.0	254.0	256.0	230.0
2.5	253.2	226.0	222.0	250.0	245.0	259.0	258.0	250.0	252.0	222.0
3	249.4	221.0	217.0	247.0	241.0	256.0	255.0	247.0	249.0	217.0
4	243.6	216.0	212.0	242.0	236.0	251.0	250.0	240.0	244.0	212.0
5	239.2	213.0	208.0	239.0	232.0	248.0	246.0	235.0	241.0	208.0
6.5	234.1	210.0	204.0	235.0	227.0	243.0	242.0	234.0	237.0	204.0
8	230.2	207.0	201.0	232.0	224.0	240.0	238.0	232.0	234.0	201.0
10	227.7	204.0	197.0	228.0	220.0	236.0	235.0	229.0	230.0	198.0
13	226.0	204.0	197.0	227.0	218.0	231.0	231.0	230.0	227.0	198.0
16	224.6	204.0	198.0	226.0	216.0	228.0	228.0	228.0	224.0	198.0
20	223.1	204.0	198.0	224.0	214.0	221.0	225.0	227.0	222.0	199.0
25	221.7	203.0	198.0	223.0	212.0	217.0	222.0	221.0	220.0	199.0
30	220.5	202.0	198.0	220.0	212.0	213.0	219.0	219.0	218.0	199.0
40	218.6	205.0	199.0	215.0	212.0	211.0	214.0	213.0	214.0	197.0
50	217.2	211.0	200.0	211.0	211.0	210.0	209.0	209.0	209.0	203.0
65	216.6	209.0	202.0	204.0	211.0	209.0	203.0	198.0	204.0	204.0
80	216.6	210.0	204.0	200.0	210.0	205.0	201.0	198.0	201.0	203.0
100	216.6	212.0	205.0	200.0	209.0	207.0	203.0	195.0	198.0	208.0
130	216.6	212.0	209.0	204.0	212.0	213.0	210.0	206.0	206.0	208.0
160	216.6	210.0	211.0	211.0	213.0	219.0	216.0	212.0	212.0	209.0
200	216.6	207.0	212.0	219.0	211.0	224.0	222.0	221.0	220.0	209.0
250	220.8	213.0	213.0	229.0	214.0	224.0	225.0	228.0	230.0	208.0
300	228.6	221.0	214.0	239.0	224.0	228.0	230.0	237.0	239.0	215.0
400	241.4	235.0	218.0	255.0	240.0	237.0	246.0	254.0	256.0	230.0
500	251.9	226.0	226.0	266.0	253.0	248.0	258.0	266.0	269.0	240.0
650	264.8	238.0	238.0	278.0	269.0	259.0	273.0	279.0	278.0	252.0
800	275.5	248.0	248.0	287.0	279.0	269.0	275.0	283.0	287.0	260.0
1000	287.4	245.0	245.0	292.0	272.0	271.0	270.0	294.0	300.0	245.0

Table A1.--Temperature profiles (continued)

TEST CASES		
60N Jan.	Point Mugu	"CRAZY"
224.2	192.0	220.0
246.2	219.4	240.0
247.5	229.6	260.0
247.8	235.6	270.0
261.2	254.3	260.0
257.9	259.1	250.0
252.8	261.2	240.0
248.1	262.1	230.0
244.0	262.4	220.0
239.4	262.2	210.0
234.7	261.4	200.0
230.9	260.3	210.0
225.2	257.6	220.0
221.3	254.7	240.0
217.4	250.2	250.0
214.9	245.7	260.0
212.8	240.0	270.0
211.3	232.1	260.0
210.8	225.4	250.0
210.8	218.0	240.0
211.6	210.9	230.0
212.7	205.7	220.0
214.8	198.9	210.0
216.4	195.5	200.0
217.8	194.2	200.0
218.2	195.6	200.0
217.8	200.0	200.0
215.6	209.1	210.0
213.4	218.6	220.0
212.1	229.9	230.0
213.0	241.4	240.0
216.6	250.2	242.0
228.0	261.7	245.0
239.5	267.4	260.0
252.1	268.8	270.0
258.4	265.1	260.0
257.5	258.0	250.0

APPENDIX B. THE 144 HOMOGENEOUS PATHS

These paths are the basis for the computations of coefficients for the polynomial representation of water-vapor transmittances. Each path corresponds to a particular mixture of water vapor and air that is characterized by its values of three parameters--total pressure, temperature, and water-vapor amount. The 144 paths comprise combinations of these parameters that span the range of conditions encountered in real atmospheres.

The 144 paths are specified by combinations of six values of pressure (i.e., P_i, i=1, 6), six values of temperature (i.e., T_j, j=1,6), and six sets of water vapor amounts (i.e., $[U]_k$,k=1,6), with each set having 12 water-vapor amounts. The six pressures and six temperatures are listed in table B1, while the six 12-element sets of water-vapor amounts appear in table B2. Table B3 lists the allowed combinations of P_i, T_j, and $[U]_k$ that comprise the 144 paths. For example, the first twelve combinations are P_1, T_1, $[U_1]_1$; P_1, T_1, $[U_2]_1$;... P_1, T_1, $[U_{12}]_1$; and the thirteenth is P_1, T_2, $[U_1]_1$.

Table B1.--The six values of pressure and temperature

Index	Pressure (mb)	Temperature (°K)
1	1000	310
2	800	290
3	500	265
4	250	225
5	100	190
6	50	220

Table B2.--The six 12-element sets of water vapor amount. Entries are water-vapor amounts in units of g/cm^2.

Element	1	2	3	4	5	6
1	23.400	6.300	1.0200	4.500×10^{-2}	6.000×10^{-3}	3.000×10^{-3}
2	14.251	4.059	0.6485	2.989×10^{-2}	9.135×10^{-3}	2.068×10^{-3}
3	8.678	2.615	0.4123	1.986×10^{-2}	2.850×10^{-3}	1.425×10^{-3}
4	5.285	1.685	0.2622	1.319×10^{-2}	1.964×10^{-3}	9.821×10^{-4}
5	3.219	1.085	0.1667	8.762×10^{-3}	1.354×10^{-3}	6.769×10^{-4}
6	1.960	0.6992	0.1060	5.820×10^{-3}	9.330×10^{-4}	4.665×10^{-4}
7	1.194	0.4505	6.738×10^{-2}	3.866×10^{-3}	6.431×10^{-4}	3.215×10^{-4}
8	0.7270	0.2902	4.284×10^{-2}	2.568×10^{-3}	4.432×10^{-4}	2.216×10^{-4}
9	0.4427	0.1870	2.724×10^{-2}	1.706×10^{-3}	3.055×10^{-4}	1.527×10^{-4}
10	0.2696	0.1205	1.732×10^{-2}	1.133×10^{-3}	2.105×10^{-4}	1.053×10^{-4}
11	0.1642	7.761×10^{-2}	1.101×10^{-2}	7.527×10^{-4}	1.451×10^{-4}	7.255×10^{-5}
12	0.1000	5.000×10^{-2}	7.000×10^{-3}	5.000×10^{-4}	1.000×10^{-4}	5.000×10^{-5}

Table B3.--The 144 paths. Each combination is a set of 12 paths corresponding to the 12 elements of $[U]_k$.

Index	Combination
1	$P_1, T_1, [U]_1$
2	$P_1, T_2, [U]_1$
3	$P_1, T_3, [U]_1$
4	$P_1, T_4, [U]_1$
5	$P_2, T_2, [U]_2$
6	$P_2, T_3, [U]_2$
7	$P_2, T_4, [U]_2$
8	$P_3, T_3, [U]_3$
9	$P_3, T_4, [U]_3$
10	$P_4, T_4, [U]_4$
11	$P_5, T_5, [U]_5$
12	$P_6, T_6, [U]_6$

(Continued from inside front cover)

NESS 61 The Measurement of Atmospheric Transmittance From Sun and Sky With an Infrared Vertical Sounder. W. L. Smith and H. B. Howell, September 1972, 16 pp. (COM-73-50020)

NESS 62 Proposed Calibration Target for the Visible Channel of a Satellite Radiometer. K. L. Coulson and H. Jacobowitz, October 1972, 27 pp. (COM-73-10143)

NESS 63 Verification of Operational SIRS B Temperature Retrievals. Harold J. Brodrick and Christopher M. Hayden, December 1972, 26 pp. (COM-73-50279)

NESS 64 Radiometric Techniques for Observing the Atmosphere From Aircraft. William L. Smith and Warren J. Jacob, January 1973, 12 pp. (COM-73-50376)

NESS 65 Satellite Infrared Soundings From NOAA Spacecraft. L. M. McMillin, D. Q. Wark, J.M. Siomkajlo, P. G. Abel, A. Werbowetzki, L. A. Lauritson, J. A. Pritchard, D. S. Crosby, H. M. Woolf, R. C. Luebbe, M. P. Weinreb, H. E. Fleming, F. E. Bittner, and C. M. Hayden, September 1973, 112 pp. (COM-73-50936/6AS)

NESS 66 Effects of Aerosols on the Determination of the Temperature of the Earth's Surface From Radiance Measurements at 11.2 m. H. Jacobowitz and K. L. Coulson, September 1973, 18 pp. (COM-74-50013)

NESS 67 Vertical Resolution of Temperature Profiles for High Resolution Infrared Radiation Sounder (HIRS). Y. M. Chen, H. M. Woolf, and W. L. Smith, January 1974, 14 pp. (COM-74-50230)

NESS 68 Dependence of Antenna Temperature on the Polarization of Emitted Radiation for a Scanning Microwave Radiometer. Norman C. Grody, January 1974, 11 pp. (COM-74-50431/AS)

NESS 69 An Evaluation of May 1971 Satellite-Derived Sea Surface Temperatures for the Southern Hemisphere. P. Krishna Rao, April 1974, 13 pp. (COM-74-50643/AS)

NESS 70 Compatibility of Low-Cloud Vectors and Rawins for Synoptic Scale Analysis. L. F. Hubert and L. F. Whitney, Jr., October 1974, 26 pp. (COM-75-50065/AS)

NESS 71 An Intercomparison of Meteorological Parameters Derived From Radiosonde and Satellite Vertical Temperature Cross Sections. W. L. Smith and H. M. Woolf, November 1974, 13 pp. (COM-75-10432)

NESS 72 An Intercomparison of Radiosonde and Satellite-Derived Cross Sections During the AMTEX. W. C. Shen, W. L. Smith, and H. M. Woolf, February 1975, 18 pp. (COM-75-10439/AS)

NESS 73 Evaluation of a Balanced 300-mb Height Analysis as a Reference Level for Satellite-Derived soundings. Albert Thomasell, Jr., December 1975, 25 pp. (PB-253-058)

NESS 74 On the Estimation of Areal Windspeed Distribution in Tropical Cyclones With the Use of Satellite Data. Andrew Timchalk, August 1976, 41 pp. (PB-261-971)

NESS 75 Guide for Designing RF Ground Receiving Stations for TIROS-N. John R. Schneider, December 1976, 126 pp. (PB-262-931)

NESS 76 Determination of the Earth-Atmosphere Radiation Budget from NOAA Satellite Data. Arnold Gruber, November 1977, 31 pp. (PB-279-633)

NESS 77 Wind Analysis by Conditional Relaxation. Albert Thomasell, Jr., January 1979.

NESS 78 Geostationary Operational Environmental Satellite/Data Collection System. July 1979, 86 pp. (PB-301-276)

NESS 79 Error Characteristics of Satellite-Derived Winds. Lester F. Hubert and Albert Thomasell, Jr. June 1979, 44 pp. (PB-300-754)

NESS 80 Calculation of Atmospheric Radiances and Brightness Temperatures in Infrared Window Channels of Satellite Radiometers. Michael P. Weinreb and Michael L. Hill, March 1980, 43 pp. (PB80 208-119)

NESS 81 Improved Algorithm for Calculation of UTM and Geodetic Coordinates. Jeff Dozier, September 1980, 21 pp. (PB81 132680)

NESS 82 The Effect of Precipitation on Microwave Soundings in Low Latitudes. Lester F. Hubert, Norman C. Grody, Andrew Timchalk, and William C. Shen, April 1981, 34 pp. (PB81 225062)

NESS 83 Atmospheric Sounding User's Guide. Adolf Werbowetzki, ed., April 1981, 82 pp. (PB81 230476)

NESS 84 Use of NOAA/AVHRR Visible and Near-Infrared Data for Land Remote Sensing. Stanley R. Schneider, David F. McGinnis Jr., James A. Gatlin, September 1981.

NOAA SCIENTIFIC AND TECHNICAL PUBLICATIONS

The National Oceanic and Atmospheric Administration was established as part of the Department of Commerce on October 3, 1970. The mission responsibilities of NOAA are to assess the socioeconomic impact of natural and technological changes in the environment and to monitor and predict the state of the solid Earth, the oceans and their living resources, the atmosphere, and the space environment of the Earth.

The major components of NOAA regularly produce various types of scientific and technical information in the following kinds of publications:

PROFESSIONAL PAPERS — Important definitive research results, major techniques, and special investigations.

CONTRACT AND GRANT REPORTS — Reports prepared by contractors or grantees under NOAA sponsorship.

ATLAS — Presentation of analyzed data generally in the form of maps showing distribution of rainfall, chemical and physical conditions of oceans and atmosphere, distribution of fishes and marine mammals, ionospheric conditions, etc.

TECHNICAL SERVICE PUBLICATIONS — Reports containing data, observations, instructions, etc. A partial listing includes data serials; prediction and outlook periodicals; technical manuals, training papers, planning reports, and information serials; and miscellaneous technical publications.

TECHNICAL REPORTS — Journal quality with extensive details, mathematical developments, or data listings.

TECHNICAL MEMORANDUMS — Reports of preliminary, partial, or negative research or technology results, interim instructions, and the like.

Information on availability of NOAA publications can be obtained from:

ENVIRONMENTAL SCIENCE INFORMATION CENTER (D822)
ENVIRONMENTAL DATA AND INFORMATION SERVICE
NATIONAL OCEANIC AND ATMOSPHERIC ADMINISTRATION
U.S. DEPARTMENT OF COMMERCE

6009 Executive Boulevard
Rockville, MD 20852

NOAA--S/T 81-248